ABSTRACT

Title of Thesis: ROLE OF ACID SPHINGOMYELINASE IN ICAM-1/NHE1-DEPENDENT ENDOCYTOSIS: IMPLICATIONS IN LEUKOCYTE TRANSMIGRATION

Daniel Serrano, Master of Science 2010

Thesis directed by: Professor Silvia Muro
Fischell Department of Bioengineering, Clark School of Engineering, and Institute for Bioscience and Biotechnology Research

Engagement of intercellular adhesion molecule-1 (ICAM-1) on endothelial cells (ECs) by anti-ICAM coated beads generates vesiculization via cell adhesion molecule (CAM)-mediated endocytosis, a clathrin-/caveolae-independent pathway involving Na^+/H^+ exchanger 1 (NHE1). ICAM-1 itself plays a key role in transendothelial migration (TEM) of leukocytes, particularly via the transcellular route. This involves endothelial endocytic vesicles that coalesce into transmigration pores, through which leukocytes transmigrate without disrupting EC junctions. The contribution of CAM-mediated endocytosis to the formation of docking sites and vesicular structures supporting TEM was explored in this study. Results show that the ICAM-1/NHE1-dependent CAM-mediated pathway associates with acid sphingomyelinase and ceramide. This supports plasmalemma deformability and cytoskeleton rearrangement, bridging these events to the formation of endothelial docking structures and vesicles involved in leukocyte transmigration.

ROLE OF ACID SPHINGOMYELINASE IN ICAM-1/NHE1-DEPENDENT ENDOCYTOSIS: IMPLICATIONS IN LEUKOCYTE TRANSMIGRATION

by

Daniel Serrano

Thesis submitted to the Faculty of the Graduate School of the
University of Maryland, College Park, in partial fulfillment
of the requirements for the degree of
Master of Science
2010

Advisory committee:
Professor Silvia Muro, chair
Professor Volker Briken
Professor Wenxia Song
Professor Li Zhang

Acknowledgements

I would like to thank my advisor, Dr. Silvia Muro for her invaluable support and guidance during the course of this project. I acknowledge Dr. Ming Meng, Dr. Carmen Garnacho, Rishi Chadha, and Dr. Tridib Bhowmick for their help and contribution to this project. Finally, I thank the support of my family and friends as I continue forward with my Ph.D. research.

My graduate studies during the course of this work were supported by a Bridge to the Doctorate Fellowship and a Graduate Research Fellowship, both from the National Science Foundation. Laboratory funds included the Minta Martin Foundation, American Heart Association Beginning Grant-in-Aid 09BGIA2450014 and National Institutes of Health R01 HL098416.

Table of contents

List of tables

List of figures

List of abbreviations

ASM, Acid sphingomyelinase
CAM, Cell adhesion molecule
Cdx, Methyl-β-cyclodextrin
D1-D5, Domains 1 through 5 of ICAM-1
EC, Endothelial cell
EIPA, 5-(*N*-ethyl-*N*-isopropyl)amiloride
ERM, Ezrin-radixin-moesin
H-7, 1-(5-isoquinolinylsulfonyl)-2-methyl-piperzine
HUVEC, Human umbilical vein endothelial cell
ICAM-1, Intercellular adhesion molecule-1
LFA-1, Lymphocyte function-associated antigen 1
M6PR, Mannose-6-phosphate receptor
MAPK, Mitogen-activated protein kinase
MDC, Monodansylcadaverine
MLEC, Mouse lung endothelial cell
NHE1, Na^+/H^+ exchanger 1
PECAM-1, Platelet-endothelial cell adhesion molecule-1
PI3K, Phosphatidylinositol 3-phosphate kinase
PMN, Polymorphonuclear leukocyte
ROCK, Rho-dependent kinase
ROS, Reactive oxygen species
SDF-1α, Stromal cell-derived factor 1-alpha
SEM, Scanning electron microscopy
TEM, Transendothelial migration
TNFα, Tumor necrosis factor α
VCAM-1, Vascular cell adhesion molecule-1
VLA-4, Very late antigen 4
WBC, White blood cell

Chapter 1: Background and significance

1.1. Intercellular adhesion molecule-1 (ICAM-1). ICAM-1 is a type I transmembrane glycoprotein of the immunoglobulin superfamily expressed mainly on the plasmalemma of endothelial cells (ECs)[1,2]. Its expression is constitutive, but upregulated during inflammatory conditions by agents such as tumor necrosis factor α (TNFα)[3]. The extracellular region of ICAM-1 consists of 5 discrete immunoglobulin-like domains (D1 at the N-terminus, through D5) arranged linearly in a rod-like conformation that extends 20 nm away from the plasmalemma[4,5]. As such, ICAM-1 is displayed in a manner suitable for its function as an adhesive receptor for leukocyte integrins $\alpha_L\beta_2$ and $\alpha_M\beta_2$ which can interact with D1 and D3, respectively[6,7] (Fig. 1).

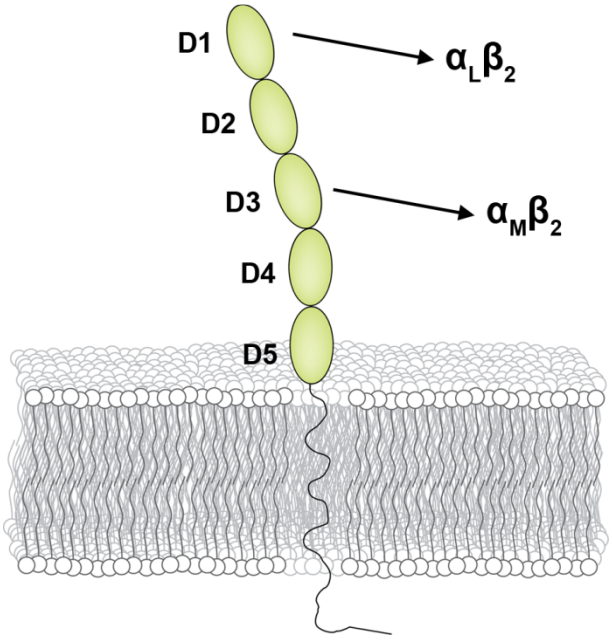

Figure 1. Structure of ICAM-1. Intercellular adhesion molecule-1 (ICAM-1) on the plasma membrane. Domains (D) 1 through 5 are found on the N-terminal extracellular side of the plasmalemma. A transmembrane domain is followed by a C-terminal short cytosolic tail. Binding sites for leukocyte integrins are on D1 and D3.

The cytosolic tail of ICAM-1 is short, consisting of 28 residues[8], and lacks conventional protein-protein interaction domains. However, the sequence contains several positively-charged residues and a tyrosine residue, which account for its protein-binding and signaling activities[9-15]. In particular, most proteins that bind the cytosolic tail of ICAM-1 serve as cytoskeleton adaptors: α-actinin[11], β-tubulin[12], and erzin[16]. Radixin and moesin, the two other members of the ezrin-radixin-moesin (ERM) family of actin adaptors, have been found to colocalize with ICAM-1[17,18]. These interactions with members of the cytoskeleton or cytoskeleton-adaptor proteins appear to be important for ICAM-1 distribution on the plasma membrane: ICAM-1 is normally found enriched in microvillar structures, while deletion of its cytoplasmic domain shifts distribution to homogeneous on the cell surface[11,16,19]. Scanning electron microscopy (SEM) reveals that this redistribution is itself associated with a loss in microvilli structures[19]. This suggests a link between ICAM-1 and formation of membrane protrusions.

Signal transduction is also associated with the cytosolic residues of ICAM-1. Engagement of ICAM-1 at the surface of ECs using cross-linked antibodies (known as multivalent engagement/binding) activates xanthine oxidase activity, generating reactive oxygen species (ROS) that in turn activate Src-kinases[20-23]. ICAM-1 cross-linking also activates small GTPase Rho[17,18,24,25], RhoA[18] and perhaps other Rho proteins[15,20], and mitogen-activated protein kinases (MAPK)[23,26]. In turn, p38 MAPK phosphorylates HSP27 and this leads to cytoskeletal rearrangement[27]. Along with MAPK, cytoskeleton-associated proteins ezrin, cortactin, focal adhesion kinase, paxillin, and p130Cas are also phosphorylated downstream of Src[5,20,22,23], consistent with multiple reports that cross-linking ICAM-1 elicits rearrangement of the actin cytoskeleton[28-31]. Wittchen has

recently summarized the current signaling paradigms associated with ICAM-1 signaling[32]. These events occur in parallel to ICAM-1 redistribution to detergent-resistant membrane fractions, an event likely to be important for signaling through ICAM-1. For instance, Src activation seems to depend on Src-homology domain 2 containing phosphatase 2, which binds to ICAM-1 upon cross-linking and entry into detergent-resistant membrane fractions[9,10]. Specialized lipid domains might serve as rigid platforms for localized maintenance of ICAM-1-dependent signaling events and cytoskeletal remodeling[33]. Hence, it is expected that the physiological functions of ICAM-1 will be associated with such signaling pathways, specialized platforms, and the membrane protein/lipid composition and morphological changes associated with these domains.

1.2. Leukocyte transendothelial migration. Recruitment of leukocytes to inflammatory sites is described as a sequential series of events that results in transendothelial migration (TEM), or crossing of the EC barrier[34,35]. In this model, leukocytes are recruited by tethering, followed by rolling interactions, strong adhesion, lateral crawling, and TEM, which can occur through a paracellular or a transcellular route[32,34,36] (Fig. 2). The initial steps of tethering and rolling involve the interaction of leukocyte L-selectin or EC E- and P-selectins with P-selectin glycoprotein ligand 1 and other glycosylated ligands expressed on either leukocytes or ECs[34,37-39]. Although rolling can also be supported by leukocyte integrin interactions with EC surface proteins[34,40,41], these binding events are crucial for arrest and firm adhesion[42,43]. The most commonly studied interactions in firm adhesion are those of leukocyte integrins $\alpha_L\beta_2$ (lymphocyte function-associated antigen 1, LFA1)

and $\alpha_4\beta_1$ (very late antigen 4, VLA-4) with ICAM-1 and vascular cell adhesion molecule-1 (VCAM-1), respectively[44,45].

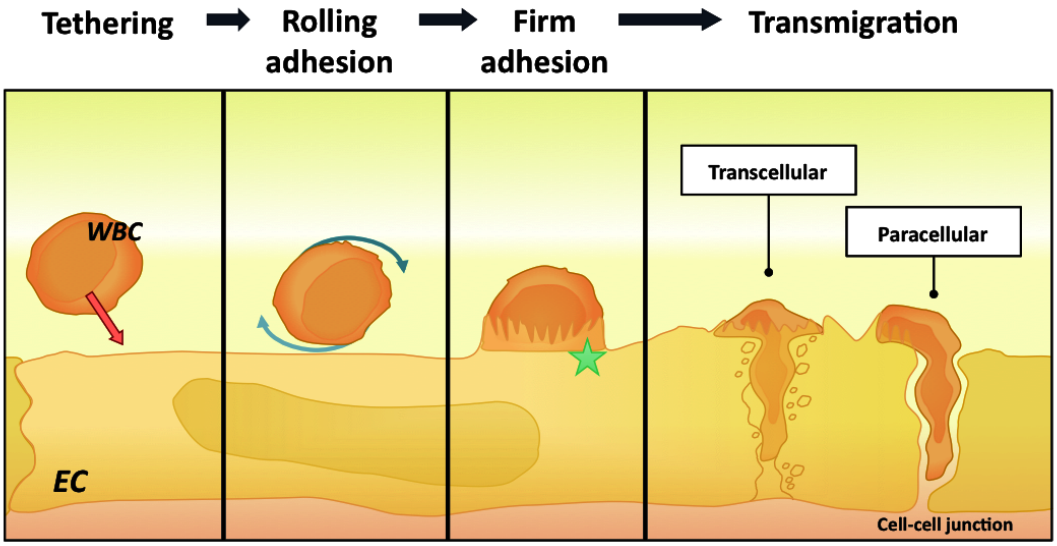

Figure 2. Main steps of leukocyte recruitment at the endothelium and transendothelial migration. Leukocytes undergo selectin-mediated tethering and rolling, followed by integrin-mediated firm adhesion, which leads to formation of endothelial docking structures (star). After firm adhesion, crawling (not shown) involves lateral migration of leukocytes to sites suitable for transmigration. Finally, transendothelial migration can occur by two means. The transcellular path involves tractive forces by docking structures, and EC vesicular fusion into transcellular pores. The paracellular path involves opening of endothelial cell-cell junctions and crossing of the endothelium through these junction openings.

Regarding transmigration, paracellular TEM involves dissociation of cell junctions between ECs, and passage of leukocytes in between opened junctions[34,46]. Transcellular TEM is independent of junction opening, where a leukocyte moves across the body of an individual EC in a process that involves fusion of endothelial vesicles into a so-called transcellular pore, through which leukocytes migrate[47-50].

TEM features notable membrane changes at the protein/lipid composition and morphological levels in both leukocytes and the EC plasmalemma: Following arrest, leukocytes crawl laterally on the surface of ECs, which changes leukocyte morphology

from round to flattened[19,51,52]. Along with this, leukocytes extend protrusions (~0.2-1 μm in diameter and up to several microns in length[53]) against the plasmalemma of ECs, which is thought to allow leukocytes to probe for sites suitable for transmigration[47,53]. Simultaneously, ECs extend protrusions around leukocytes, which form a structure known as the transmigratory cup, or docking structure[48,54,55]. The formation of this structure, which is enriched in ICAM-1, likely due to profuse LFA-1-ICAM-1 interactions, is associated with rearrangement of the actin cytoskeleton to form stress fibers, and depends on the cytosolic tail of ICAM-1[19,55,56]. The maintenance of these large regions of specific molecular enrichment is associated with protein/lipid rearrangement to form specialized lipid domains at the plasma membrane that allow for ICAM-1-dependent signaling events. This is manifested in the enrichment of ICAM-1, VCAM-1, tetraspanin CD9, actin, RhoG, ezrin, and moesin[48,54-56], and a redistribution of ICAM-1 to detergent-resistant membrane fractions[57].

Accompanying the formation of transmigratory cups is the generation of EC plasma membrane vesicles of 200 nm to 1 μm in diameter that coalesce into larger structures, with the eventual formation of a pore that transverses the entire EC body, through which leukocytes transmigrate[49,53]. This structure is known as the transcellular pore and can be as large as 6 μm in diameter[53]. Although some data suggest the involvement of caveolar endocytosis and/or the related vesiculo-vacuolar organelle during this phenomenon[49], some reports have shown no or partial association between the transcellular pore and other structures associated with TEM and caveolin[48,53,58]. Thus, the nature and regulation of these dynamic vesicular events and structures remains unclear.

1.3. ICAM-1 in leukocyte transendothelial migration. Leukocytes bind ICAM-1 through their integrins LFA-1 and $\alpha_M\beta_2$ (macrophage-1 antigen, Mac-1)[6,44,59]. Initially, this interaction was characterized as exclusively adhesive, particularly at the TEM stage of firm adhesion, but signaling functions have now been attributed to ICAM-1 binding by leukocytes. Since a single leukocyte exhibits multiple copies of these integrins, it can engage multiple copies of ICAM-1. Thus, signaling events observed during ICAM-1 multivalent binding by antibodies, as described in Section 1.2, match with those associated with leukocyte binding and TEM[60]. For instance, inhibition of Rho activity diminishes lymphocyte migration through brain cells in an ICAM-1-dependent manner[24]. Binding of polymorphonuclear leukocytes (PMNs) to ECs increases intracellular Ca^{2+}, and disallowing Ca^{2+} increase prevents transmigration but not binding[61]. PMN adhesion to ECs induces rearrangement of the actin cytoskeleton[30,31], prevented by inhibition of p38 MAPK[26]. Finally, cortactin phosphorylation is essential for leukocyte TEM[62].

More specifically, the role of ICAM-1 in leukocyte transcellular TEM has become well recognized. TNFα activation of ECs to induce ICAM-1 overexpression increases the percentage of PMNs that migrate using the transcellular route[50]. Further, blocking or deleting the cytoplasmic domain of ICAM-1 reduces transcellular TEM events, suggesting that transcellular migration depends on ICAM-1 signaling and/or association with actin[50]. During transcellular TEM, ICAM-1 becomes internalized and undergoes transcytosis to the basal membrane of ECs[49], which is likely a manifestation of transcellular pore aperture, as regions where podosomes probe EC membrane and transcellular pores form, are enriched in ICAM-1.

Interestingly, formation of plasmalemma engulfing structures, invaginations and coalescing vesicles, as well as upstream signaling and cytoskeletal restructuring observed during ICAM-1 engagement by antibodies are reminiscent of the events elicited during ICAM-1-specific leukocyte binding to ECs prior to transmigration. This points to a possible role for ICAM-1-mediated formation of endocytic vesicles during leukocyte TEM.

1.4. CAM-mediated endocytosis. As described above, ICAM-1 serves as an adhesive molecule for leukocytes during inflammation, and subsequent work revealed signaling properties associated with this function. Studies on the use of ICAM-1 for endothelium-targeted delivery of therapeutics led to the discovery of its role as an endocytic receptor[29]. Cell adhesion molecule (CAM)-mediated endocytosis is a non-classical endocytic pathway (Table 1) elicited upon engagement of multiple copies of ICAM-1 (Fig. 3). Multivalent engagement can be achieved by the interaction between antibody-coated micro- or nanoparticles and ICAM-1 on the EC surface, which is followed by Na^+/H^+ exchanger 1 (NHE1)-dependent endocytosis of particles and intracellular trafficking to early endosomes and then lysosomes[29,63,64]. Recent studies in our group have shown that a fraction of objects internalized by CAM-mediated endocytosis undergo transcytosis in epithelial cells[65].

Table 1. Comparison of endocytic pathways.

	CR-mediated phagocytosis	FcR-mediated phagocytosis	Macropinocytosis	Caveolae-mediated endocytosis	Clathrin-mediated endocytosis	CAM-mediated endocytosis	CME Differs from
Internalize particles > 1um	+	+	+	-	-	+	Cav, Clat
Receptor-mediated	+	+	-	+	+	+	M
Dynamin-2	+	+	-	+	+	+	M
NHE	-	-	+	-	-	+	C, F, Cav, Clat
PKC	+	+	+	+	+	+	n
Actin	+	+	+	+	+	+	n
Actin cup	+	+	+	-	-	-	C, F, M
Microtubules	+	-	+	+	+	-	C, M, Cav, Clat
Src kinase	-	+	+	+	+	+	C
PI3 kinase	+	+	+	?	-	-	C, F, M
Rho/ROCK	+	-	?	?	?	+	F
Colocalization with caveolin-1	-	-	-	+	-	-	Cav
Sensitive to MDC/K^+ depletion	-	-	-	-	+	-	Clat
Sensitive to filipin/genistein	?	?	-	+	-	-	Cav
Sensitive to LatA/CytD	+	+	+	+	+	+ (LatA) / - (CytD)	C, F, M, Cav, Clat

Adapted from Caron and Hall[67], and Muro et al.[29]

+, required for uptake/event observed; –, not required for uptake/event not observed; ?, no definitive data found in the literature/not previously tested.
MDC, monodansylcadaverine; LatA, latrunculin A; CytD, cytochalasin D; C, complement receptor (CR)-mediated phagocytosis; F, FcR-mediated phagocytosis; M, macropinocytosis; Cav, caveolae-mediated endocytosis; Clat, clathrin-mediated endocytosis; CME, CAM-mediated endocytosis; n, none.

Similar to clathrin- and caveolae-dependent endocytosis, CAM-mediated endocytosis is dynamin-dependent[29]. However, fluorescently labeled anti-ICAM beads do not colocalize with clathrin heavy chain or caveolin-1 during the process of internalization or intracellular trafficking[29]. This is confirmed by transmission electron microscopy images of mouse endothelium, which show that anti-ICAM beads are contained in EC invaginations and vesicles not associated with typical morphological features of these two classical endocytic pathways, such as caveolar pits and clathrin coats[66]. Further, pharmacological inhibitors of caveolae- (filipin and genistein) or clathrin-mediated (K^+ depletion and monodansylcadaverine, MDC) endocytosis do not inhibit internalization elicited by multivalent binding of ICAM-1[29].

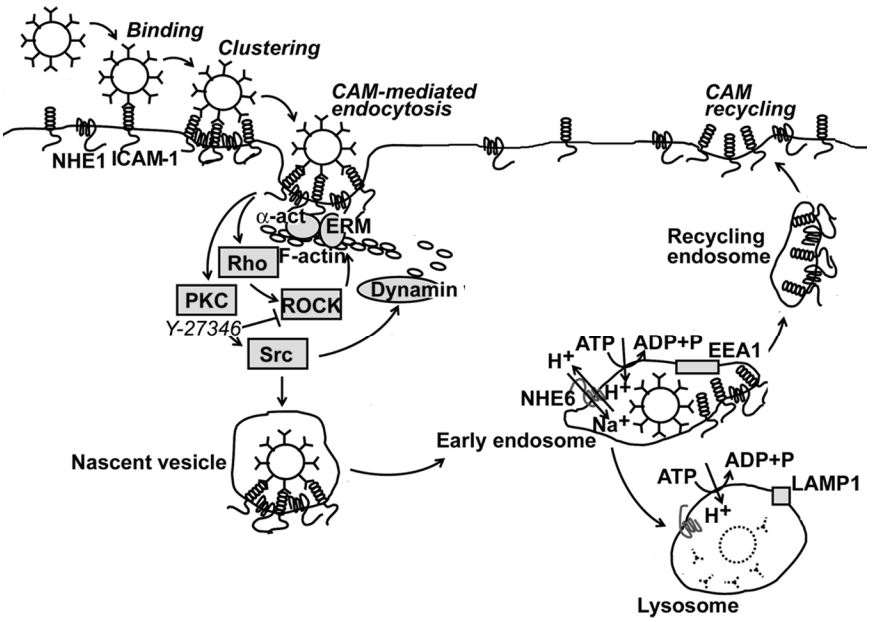

Figure 3. CAM-mediated endocytosis and signaling. CAM-mediated endocytosis is initiated upon multivalent binding of ICAM-1 by anti-ICAM-coated particles. ICAM-1 engagement elicits the recruitment of NHE1, which is itself an adaptor of the actin cytoskeleton. Signaling through Rho/ROCK, PKC, and Src elicits dynamin-dependent endocytosis. Internalized vesicles fuse into early endosomes, where ICAM-1 dissociates from anti-ICAM beads, and recycles back to the plasma membrane. Early endosomes maturate/fuse with lysosomes in an NHE6-dependent manner. The final trafficking destination of beads is the lysosome. Not shown is the alternative pathway of transcytosis, which has been shown to occur in epithelial cells[65].

Due to the close association between CAM-mediated endocytosis and the actin cytoskeleton, this pathway shares certain features with macropinocytosis and phagocytosis, in particular protein kinase C (PKC) dependence, as PKC inhibitors bisindolylmaleimide-1 (BIM-1) and 1-(5-isoquinoline-sulphonyl)-2-methylpiperazine (H-7) reduce, and PKC stimulator phorbol 12-myristate 13-acetate (PMA, applied in a short-time incubation) increases, internalization of anti-ICAM beads[29]. However, CAM-mediated endocytosis does not exhibit the formation of actin cups or membrane ruffling, as the two other pathways[29]. Furthermore, CAM-mediated endocytosis is independent of microtubules for internalization to occur, unlike macropinocytosis, and of phosphatidylinositol 3-phosphate kinase (PI3K) signaling, unlike phagocytosis[29]. As observed with cross-linked antibodies, which also multivalently engage ICAM-1, multivalent engagement of ICAM-1 with anti-ICAM beads leads to particular signaling events. CAM-mediated endocytosis is associated with Rho-dependent kinase (ROCK), PKC, and Src kinase[29], culminating in remodeling of the actin cytoskeleton into stress fibers. Despite considerable characterization of CAM-mediated endocytosis, this pathway has not been studied in the context of its potential physiological function. Thus, it is still unknown if this pathway of endocytosis is relevant to the biological function of ICAM-1.

1.5. Scope of the research. Based on the evidence presented, this project aims at investigating the possible association between CAM-mediated endocytosis and leukocyte transmigration. The main hypothesis claims that events observed during ICAM-1 engagement on the endothelium, which result in CAM-mediated formation of vesicles, will also occur during and contribute to transmigration across the endothelium by leukocytes.

Chapter 2: Materials and methods

2.1. Antibodies and reagents. Monoclonal antibodies to the extracellular domain of human or mouse ICAM-1 were R6.5 and phycoerythrin-conjugated LB-2 (Santa Cruz Biotechnology, Inc., Santa Cruz, CA), or YN1, respectively[64,66]. Monoclonal antibodies to mouse platelet-endothelial cell adhesion molecule-1 (PECAM-1), or human VCAM-1, VLA-4, LFA-1 integrin, or ceramide were from BD Biosciences (Franklin Lakes, NJ), EMD Chemicals (Gibbstown, NJ), Millipore (Billerica, MA), Santa Cruz Biotechnology, Inc. (Santa Cruz, CA), and Sigma-Aldrich, Inc. (Saint Louis, MO). Polyclonal antibodies to human acid sphingomyelinase (ASM), tetraspanin CD9, NHE1 or ganglioside GM1 were from Santa Cruz Biotechnology, Inc. (Santa Cruz, CA) and EMD Chemicals (Gibbstown, NJ). Secondary antibodies were from Jackson Immunoresearch Laboratories, Inc. (West Grove, PA) and Santa Cruz Biotechnology, Inc. (Santa Cruz, CA). Polystyrene-latex beads were from Polysciences, Inc. (Warrington, PA). BODIPY® FL C_{12}-sphingomyelin and Texas Red-labeled phalloidin were from Molecular Probes, Inc. (Eugene, OR). All other reagents were from Sigma-Aldrich, Inc. (Saint Louis, MO).

2.2. Cell culture. Human umbilical vein endothelial cells (HUVECs) purchased from Lonza Walkersville, Inc. (Walkersville, MD) were cultured in M-199 medium supplemented as described[29]. Mouse lung endothelial cells (MLECs) were isolated from wild-type C57BL/6 (The Jackson Laboratory, Bar Harbor, ME) or $ASM^{-/-}$ mice[68] (kindly provided by Dr. Edward Schuchman, Mount Sinai School of Medicine, New York, NY) by cutting lungs into 1-2 mm fragments, followed by digestion overnight at 4°C in 1 mg/mL collagenase and filtration through a 40 μm nylon mesh[69]. Cells were isolated by

incubation with anti-PECAM Mec13.3-coated Dynabeads® (Invitrogen Corporation, Carlsbad, CA) for 30 minutes at 4°C, and cultured in supplemented DMEM medium[69]. Isolation of MLEC from mice adjusted to IACUC regulations. For experiments, ECs were seeded on 1%-gelatin-coated glass coverslips or 8-μm pore Transwell® filters (Corning Inc., Lowell, MA), as indicated. Cells were treated for 16 hours with 10 ng/mL TNFα (BD Biosciences, Franklin Lakes, NJ) to induce endothelial activation and up-regulation of ICAM-1 expression.

Wild-type peripheral-blood leukocytes (herein called white blood cells, WBCs) were obtained from healthy volunteers (under IRB-approved protocols) following a standard protocol for lymphocyte isolation. Shortly, isolation was done in 0.109 M sodium citrate using density gradient centrifugation over Ficoll-Paque™ PLUS (GE Healthcare Amersham Biosciences Corp., Piscataway, NJ), followed by incubation of WBCs as non-adherent cells in RPMI-1640 supplemented with 10% fetal bovine serum (Mediatech, Inc., Manassas, VA). Non-migratory K562 erythroid leukemia cells were obtained from Sigma-Aldrich (Inc., Saint Louis, MO) and cultured in supplemented RPMI. Prior to experiments, WBCs or K562 cells were activated with 50 U/ml interleukin 2 (IL-2) for 72 hours.

2.3. Quantification of leukocyte transmigration across endothelial cell monolayers. IL-2-activated WBCs were added at 1.5-WBC to 1-HUVEC ratio to the upper chamber above a confluent monolayer of TNFα-activated HUVECs grown on 8-μm pore Transwell® filters. Recombinant lymphocyte chemoattractant stromal cell-derived factor 1-alpha (SDF-1α; R&D Systems, Inc., Minneapolis, MN) was added at 200 ng/mL to the

chamber under HUVECs. Transmigration was assessed by counting WBCs from the bottom chamber after incubation with HUVECs for 30 minutes at 37°C. For inhibition, HUVECs were pre-treated with 3 mM amiloride, which blocks CAM-mediated endocytosis, or 1 μg/mL filipin or 5 mM methyl-β-cyclodextrin (Cdx) to chelate cholesterol, and the inhibitors were maintained through the experiment. Alternatively, WBCs were pre-treated with 40 ng/μL anti-VLA-4 (to block binding to VCAM-1) or anti-LFA-1 (to block binding to ICAM-1), then washed and incubated over HUVECs.

Although transmigration of leukocytes across ECs has been shown to be enhanced under flow conditions, we used this TEM model based on Transwell® filters (which requires static conditions) to maximize sensitivity of detection: all transmigrated WBCs are accounted for in this system, whereas microscopy imaging of transmigration under flow only permits to visualize a selected endothelial area.

2.4. Imaging leukocyte adhesion and pre-transmigratory interactions with endothelial cells. IL-2-activated WBCs were stained with 4 μM green fluorescent calcein (Molecular Probes, Inc., Eugene, OR), washed, and added over TNFα-activated HUVECs growing on glass coverslips at 1.5-WBC to 1-HUVEC ratio. The cells were incubated for 30 minutes at 37°C in 200 ng/mL SDF-1α, followed by fixation with 2% cold paraformaldehyde and then washing to remove non-adhered WBCs. For inhibition, HUVECs were pre-treated with 3 mM amiloride, 1 μg/mL filipin, 5 mM Cdx, or 50 μM imipramine (to inhibit ASM), and the inhibitors were maintained through the experiment. Samples were stained after fixation using blue-fluorescent labeled-anti-ICAM (to better image the EC surface in experiments looking at WBC-EC interactions), or anti-ASM plus

a secondary antibody labeled with Texas Red (in experiments looking at ASM enrichment at the WBC-EC interface).

Samples were analyzed by phase-contrast and fluorescence microscopy (Olympus IX81, Olympus, Inc., Center Valley, PA) with a 40x oil immersion objective (UPlanApo, Olympus, Inc., Center Valley, PA). Micrographs were taken for several z-sections with an ORCA-ER camera (Hamamatsu Corporation, Bridgewater, NJ) and SlideBook™ 4.2 (Intelligent Imaging Innovations, Inc., Denver, CO). Total amount of WBCs left after washes on the EC monolayer were quantified. Rounded WBCs were scored as simply "adhered" cells and flat spread WBCs (which could have been arrested or crawling) were scored as "sampling" cells. Both adhered and sampling WBCs were additionally located at the either the EC border (in contact with the border at any extent) or away from it (EC "body"). Location of WBCs at these sites and presence of podosome-like structures in sampling WBCs were visualized in parallel by SEM.

2.5. Recruitment of molecules at sites of ICAM-1 engagement on the endothelial plasmalemma. To engage solely ICAM-1 on ECs, we adsorbed anti-ICAM on the surface of 4.5 μm diameter polystyrene-latex beads (anti-ICAM beads) as described[29,66]. Anti-mannose-6-phosphate receptor (anti-M6PR) beads and anti-VCAM-1 beads served as controls. Coated beads were incubated for 15 minutes or 30 minutes at 37ºC with control HUVECs or HUVECs treated with 5 mM Cdx, 50 μM imipramine, 3 mM amiloride, 20 μM 5-(*N*-ethyl-*N*-isopropyl)amiloride (EIPA, which inhibits NHE1[29,70,71]), 0.5 μM wortmannin (to inhibit PI3K), or 10 μM H-7 (to inhibit PKC). Beads that were not firmly bound to HUVECs were washed and cells were fixed. Cholesterol and

ganglioside GM1 were stained using 50 μg/mL filipin, and polyclonal anti-GM1 followed by a Texas Red-labeled secondary antibody, respectively, whereas sphingomyelin was visualized by incubating HUVECs with 0.2 μg/mL BODIPY®-sphingomyelin for 16 hours prior to experiments. Ceramide, ICAM-1, VCAM-1, and M6PR were immunostained as noted in Figures, using antibodies that recognize extracellular domains of these antigens and do not require cell permeabilization. Immunostainings of ASM and NHE1 were performed after permeabilization with 0.2% cold Triton X-100. Anti-ICAM on the surface of beads was detected by immunofluorescence using a secondary antibody.

Beads were first located using phase contrast microscopy. Fluorescence micrographs at these positions were then obtained in the z-axis using 0.5 μm steps in SlideBook™ 4.2, and images were analyzed using Image-Pro 6.3 (Media Cybernetics, Inc., Bethesda, MD). Enrichment of molecules in areas of the EC plasmalemma where beads were bound was visualized using pseudocolored fluorescence-intensity surface plots, which were obtained at the bead mid cross-section plane. The mid cross-section of beads is raised ~2 μm above the plasmalemma level; hence, enrichment of cellular molecules at this section shows EC membrane actively engulfing such beads. For semi-quantitative analysis of these experiments, fluorescence intensity profiles were averaged from ≥ 32 beads and enrichment of a particular molecule was calculated as fold increase (represented as Δ in graphs) in the average intensity at the mid cross-section region of engulfed beads over the average intensity of ~2 μm surrounding areas where the plasmalemma is not raised engulfing beads (“background”). In some instances, binding and/or engulfment of anti-ICAM beads by ECs was visualized in parallel by SEM.

Distribution of ASM was additionally assessed by computing the total number of ASM-positive vesicles (~100-300 nm fluorescent objects) and those located within 5 μm distance around the nucleus (perinuclear). Peripheral ASM was calculated as total − perinuclear vesicles.

2.6. CAM-mediated endocytosis of anti-ICAM beads and actin remodeling. For endocytosis experiments, TNFα-activated HUVECs, wild-type MLECs or $ASM^{-/-}$ MLECs were incubated at 37ºC with 4.5 μm anti-ICAM beads for 30 minutes to allow bead binding, followed by washing non-bound beads and incubation at 37ºC for 1 hour to allow full endocytosis. Inhibition experiments were performed in the presence of 3 mM amiloride, 50 μM imipramine, Na+-depleted ionic solution (138 mM choline chloride, 5.4 mM KCl, 1 mM $CaCl_2$, 1 mM $MgCl_2$), 0.5 μM wortmannin, or 10 μM H-7. After cell fixation, samples were stained using Texas Red-labeled goat anti-mouse IgG, which binds to anti-ICAM on non-internalized beads but does not access internalized counterparts[29]. Uptake was determined by fluorescence microscopy using Image-Pro 6.3 by counting total beads (phase contrast) and surface-bound Texas Red-fluorescent beads[29].

For actin visualization experiments, TNFα-activated HUVECs were incubated with 4.5 μm anti-ICAM beads for 30 minutes at 37ºC, followed by washing and fixation, permeabilization with 0.2% Triton X-100, and fluorescent labeling of filamentous actin using Texas Red-conjugated phalloidin.

2.7. CAM-mediated endocytosis *in vivo*. Anesthetized C57BL/6, caveolin-1$^{-/-}$ (Jackson Laboratory, Bar Harbor, ME) or ASM$^{-/-}$ mice were injected intravenously with 100 nm anti-ICAM beads instead of 4.5 μm beads to avoid capillary embolization. Induction of vesicular uptake in endothelium was assessed in lungs, to facilitate visualization due to the profuse vasculature in this organ. Mice were perfused 3 h after bead injection and lungs were isolated, fixed in 2.5% glutaraldehyde and 0.1 M sodium cacodilate buffer, and processed into 80-90 nm-thin resin-embedded sections for transmission electron microscopy[66]. Animal studies adjusted to IACUC regulations.

2.8. Statistics. Data are means ± standard error of the mean (s.e.m.) and statistical significance was determined by Student's t tests.

Chapter 3: Results

3.1. Effect of disrupting lipid domains or CAM-mediated endocytosis on leukocyte transmigration across endothelial cells. We used a model consisting of a confluent TNF-α-activated EC monolayer grown on a porous membrane through which IL-2-activated peripheral-blood lymphocytes (herein called WBCs) can transmigrate, driven by presence of chemoattractant SDF-1α in the chamber underneath ECs. Under control conditions, 77.7±2.3% WBCs underwent transmigration by 30 minutes, as opposed to total lack of transmigration of K562 cells, a non-migratory erythroid leukemia cell line used a negative control (Fig. 4A). As expected due to involvement of multiple overlapping interactions between WBCs and ECs, TEM was partially (yet significantly) inhibited by either blocking ICAM-1-binding integrin LFA-1 on WBCs using anti-LFA-1 (59.2±11.9% inhibition; Fig. 4A) or by blocking another leukocyte integrin involved in leukocyte TEM, VLA-4, which binds to VCAM-1 (41.2±5.6% inhibition; Fig. 4A). Such an effect on TEM by blocking LFA-1 or VLA-4 was independent from the WBC capacity to transverse the porous membrane in the absence of ECs (Fig. 4B) and, hence, related to specific WBC-EC interactions. These data are consistent with previous reports[72,73], validating the use of this model.

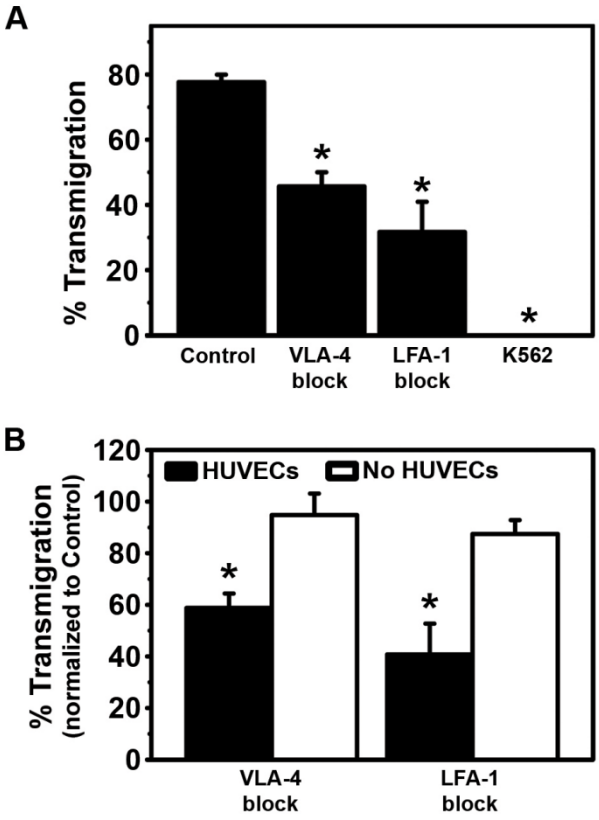

Figure 4. Model to examine transmigration of white blood cells across endothelial monolayers. (A) Transport of either peripheral-blood lymphocytes (WBCs, control) or negative control K562 cells across activated HUVEC monolayers assessed at 37ºC by counting blood cells in the bottom chamber underneath HUVECs (black bars), 30 minutes after adding blood cells to the upper chamber above HUVECs. Transmigration was alternatively performed prior to (control) or after blocking integrins LFA-1 or VLA-4 on WBCs using monoclonal antibodies. (B) Transmigration of antibody-blocked WBCs in the presence (black bars) or absence (white bars) of HUVEC monolayer, as a control. Data are normalized to control values, and represent mean and s.e.m. ($n \geq 3$ experiments). *, $P \leq 0.001$ by Student's t test.

Using this Transwell system, we observed that WBC transmigration was inhibited by Cdx (51.9±4.8% inhibition; Fig. 5A), an agent that depletes cholesterol from cells and significantly affects lipid domains, including caveolar sites. However, filipin, a drug that binds to cholesterol and can also affect caveolae-mediated pathways on these ECs[29], did not inhibit WBC transmigration (12.0±7.7% inhibition). Instead, amiloride, which affects Na^+/H^+ exchangers[70] and inhibits CAM-mediated endocytosis[29], reduced WBC transmigration even at a greater extent than Cdx (61.4±3.7% inhibition; Fig. 5A).

Although these inhibitors could affect not only ECs but potentially also WBCs, neither Cdx nor amiloride impaired the capacity of WBCs to transmigrate across the porous filter in the absence of an endothelial monolayer (Fig. 5A).

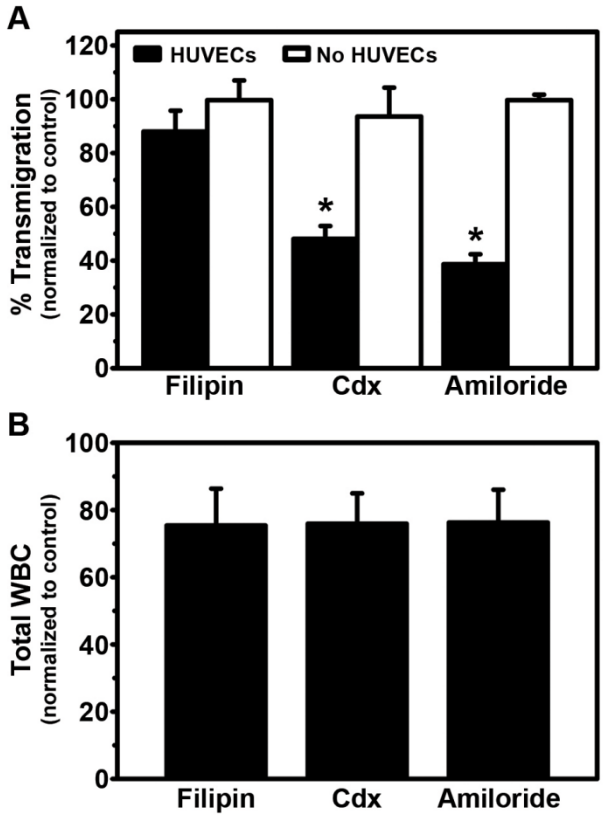

Figure 5. Endothelial binding and transmigration of white blood cells. (A) Transport of activated peripheral-blood lymphocytes (WBCs) across activated HUVEC monolayers was assessed at 37ºC by counting WBCs in the bottom chamber underneath HUVEC 30 minutes after adding WBCs to the upper chamber above HUVECs (black bars). Absence of HUVEC monolayer was a control (white bars). Transmigration was performed in the absence (control) or presence of filipin, methyl-β-cyclodextrin (Cdx) or amiloride. (B) Binding of activated WBCs (pre-stained with green fluorescent calcein) to activated HUVECs growing on glass coverslips was determined after co-incubation for 30 minutes at 37ºC in control medium or medium containing filipin, Cdx or amiloride, followed by washing to remove WBCs not firmly bound to HUVECs, and fluorescence microscopy (black bars). Data are normalized to control values, and represent mean and s.e.m. ($n \geq 3$ experiments). *, $P \leq 0.001$ by Student's t test.

Also a as a control, a parallel experiment using WBCs labeled with green-fluorescent calcein and ECs growing on coverslips (to avoid confounding results of transmigration)

showed no effect of Cdx or amiloride on WBC binding to ECs, as shown after several rounds of washing (Fig. 5B). These results agree with previous works suggesting a role for lipid domains (and possibly caveolar pathways) on TEM[49,57,74]. In addition, TEM inhibition by amiloride but not filipin corresponds well with the inhibition pattern observed for endocytosis of anti-ICAM beads by ECs[29], which agrees with a potential role for CAM-mediated endocytosis in leukocyte transmigration.

3.2. Lipid domains and CAM-mediated endocytosis in pre-transmigration interactions between leukocytes and endothelial cells. A possible contribution of CAM-mediated endocytosis to leukocyte TEM could be that of helping to regulate dynamic formation of pre-transmigratory surface invaginations and/or engulfing structures observed on ECs at the interface with leukocytes that sample the endothelial surface in search for sites optimal for transmigration[19,48,50,55,56]. To explore whether this is the case, we used the fluorescence microscopy model described in Figure 5B and looked at green-fluorescent WBCs that remained bound to ECs after several rounds of washing (firm adhesion). WBCs displaying a round morphology were scored as simply "adhered" cells, while flat, spread WBCs (which may be arrested, crawling laterally, or undergoing transmigration) were scored as "sampling" cells. Presence of WBC podosomes and related structures interacting with ECs surface were confirmed in such sampling cells by SEM (Fig. 6A, top panel). As shown in Figure 6B, 69.3±2.3% WBCs were sampling the EC surface in this model, whereas 30.7 ±10.0 % WBCs were simply adhered to ECs.

Furthermore, using phase-contrast and fluorescence imaging of the EC surface permitted us to better distinguish between sampling WBCs located at EC borders versus those away

from borders (herein called EC “body”; see partial engulfment of a WBC by the EC plasmalemma at this site; black arrowheads in Figure 7A). These locations were also verified by SEM (Fig. 6A, bottom panel). As shown in Figure 6C, sampling WBCs were equally distributed between the EC body and the EC border (53.4±4.0% and 46.6±4.0%, respectively) and 71.2±3.5% of all WBCs located at the EC body were sampling WBCs (Fig. 6D). Although sampling WBCs do not represent those that fully migrate across ECs, these results are in well agreement with data published on transmigrating leukocytes[50,72,73]. This suggests that most of these sampling interactions between WBCs and ECs can correspond to pre-transmigratory events, half of which may occur transcellularly at EC body locations.

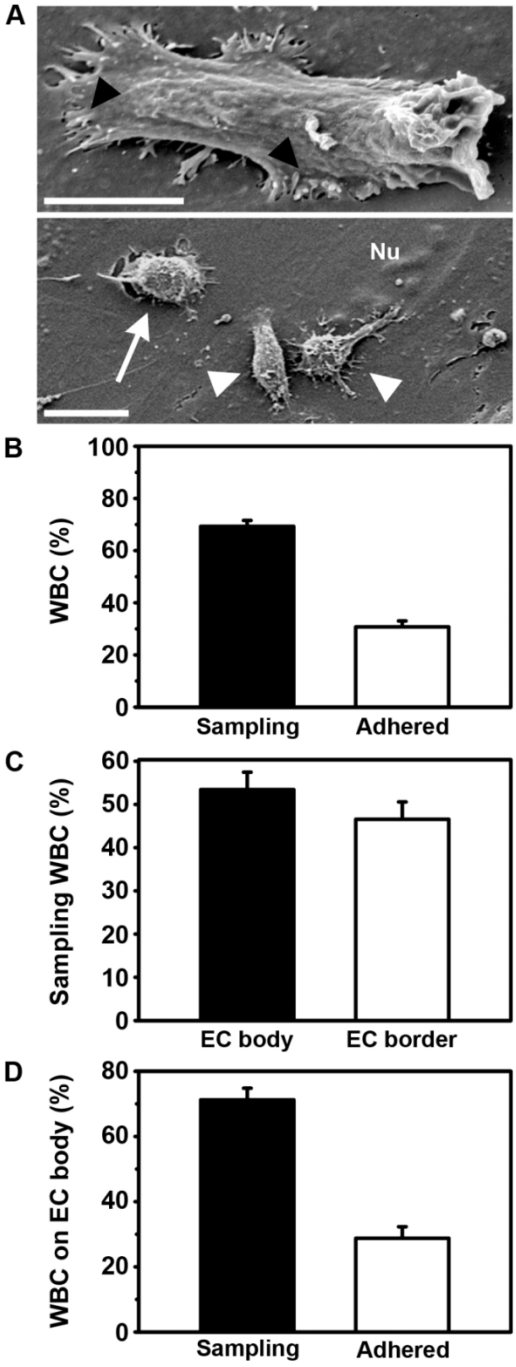

Figure 6. Model to examine pre-transmigratory interaction of white blood cells and endothelial cells. Interaction of activated peripheral-blood lymphocytes (WBCs) with activated HUVECs after incubation for 30 minutes at 37ºC. (A) Scanning electron microscopy of WBCs interacting with HUVECs. Black arrowheads in the top panel show WBC podosomes and related "sampling" structures at the interface with HUVECs. Scale bar = 5 μm. The bottom panel shows WBCs located at the EC border (arrow) or away from it (EC body; white arrowheads) Nu = Nucleus. Scale bar = 10 μm. (B-D) WBCs pre-stained with green fluorescent calcein and observed by fluorescence microscopy on HUVECs. (B) Round WBCs were scored as "adhered" cells (white bars) and spread WBCs were scored as "sampling" cells (black bars). (C) Spatial distribution of sampling WBCs at either the EC body (black bars) or the EC border (white bars). (D) Fraction of sampling WBCs (black bars) versus adhered WBCs (white bars) within those located at the EC body. Data represent mean and s.e.m. ($n \geq 30$ WBCs).

In accord with our previous set of experiments (Fig. 5), Cdx and mainly amiloride, but not filipin, reduced the number sampling WBCs (80.5±6.8%, 63.8±7.3% and 108.7±8.6% of control, respectively; Fig. 7B). In particular, Cdx and amiloride shifted the number of sampling WBCs at the EC border over the EC body (124.9±17.1% over 78.3±14.9% for Cdx and 139.6±34.1% over 65.5±29.7% for amiloride; Fig. 7C). Regarding only WBCs located at the EC body, Cdx and amiloride decreased sampling WBCs (71.5±14.6% and 56.0±27.5% of control) and increased the number of WBCs simply adhered (170.5±36.2% and 209.1±68.1% of control; Fig. 7D). Hence, this set of experiments suggests a main role for lipid domains and CAM-mediated endocytosis at the interface between leukocytes and ECs predominantly in areas away from the EC border.

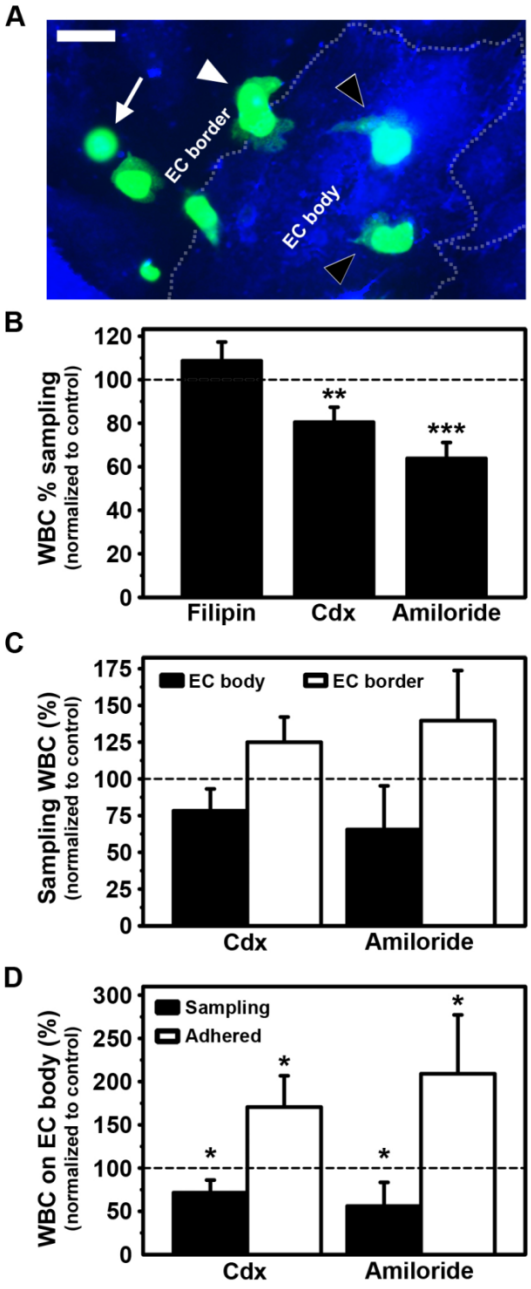

Figure 7. Pre-transmigratory interaction of white blood cells and endothelial cells. Interaction of activated peripheral-blood lymphocytes (WBCs, pre-stained with green fluorescent calcein) with activated HUVECs growing on glass coverslips was determined after co-incubation for 30 minutes at 37ºC in control medium or medium containing filipin, methyl-β-cyclodextrin (Cdx) or amiloride. WBCs not firmly adhered to HUVECs were washed, followed by fixation, immunostaining of ICAM-1 in blue, and analysis by fluorescence microscopy. (A) The image shows an example of flat spread WBCs scored as "sampling" (arrowheads, black for EC body and white for EC border), compared to rounded WBCs scored as simply "adhered" (arrow). Cell borders are indicated by semi-transparent dashed lines. Scale bar = 10 μm. (B) Percent of sampling WBCs on HUVECs (black bars). (C) Spatial distribution of sampling WBCs, scored as occurring at either the EC body (black bars) or the EC border (white bars). (D) Fraction of sampling WBCs (black bars) versus simply adhered WBCs (white bars) within those located at the EC body. Data are normalized to control values (horizontal dashed lines) and represent mean and s.e.m. ($n \geq 30$ WBCs). *, $P \leq 0.05$; **, $P \leq 0.01$; ***, $P \leq 0.001$ by Student's t test.

3.3. Association of lipid domains and the sphingomyelin/ceramide pathway with endothelial docking structures induced by ICAM-1 engagement. Endothelial engulfment of leukocytes at lipid raft-like, ICAM-1-rich docking structures occurs in association with leukocyte adhesion to the endothelium and TEM, including those processes that involve transcellular pores[19,48,55,56]. However, experiments using leukocytes involve engagement of multiple adhesion molecules on the endothelial plasmalemma. Also, inhibitors present in the cell medium during experiments may affect both EC and leukocyte counterparts. Therefore, to focus on events that occur on ECs and to better correlate engagement of ICAM-1 with lipid domains at the EC surface, we used polymer beads coated with multiple copies of an antibody against ICAM-1 (anti-ICAM beads). This reductionist, yet valuable, tool has been previously used for inducing on ECs processes similar to those elicited by leukocyte adhesion[33,56,73] and has been extensively used in the context of the CAM-mediated pathway[29,64,66,71].

Fluorescence microscopy at different focal planes on the z-axis (Fig. 8A) showed that, within 15 minutes incubation, anti-ICAM beads (immunostained in green FITC) bound to ECs and were engulfed by ICAM-1-enriched membrane protrusions (immunostained in Texas Red). SEM (Fig. 8B) confirmed that bead engulfment areas were morphologically similar to endothelial docking structures observed during leukocyte TEM[48,55,74]. Also validating this model, analysis of fluorescence intensity at the bead mid cross-section region showed that sites of bead engulfment by ICAM-1 engagement were enriched in tetraspanin CD9 (Fig. 8C), as reported for leukocytes[74].

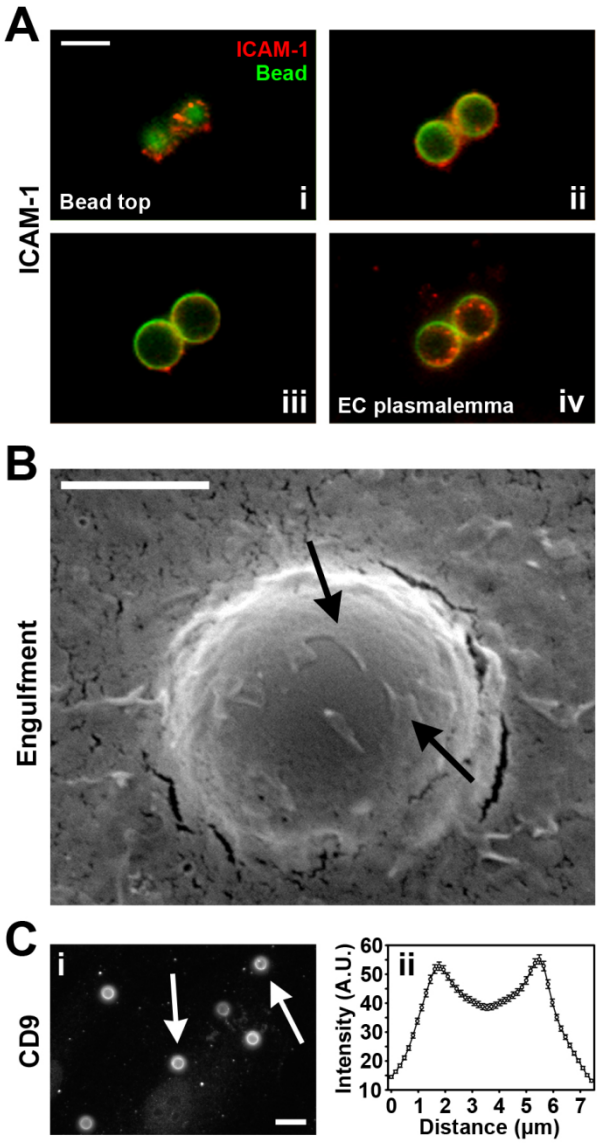

Figure 8. Induction of endothelial docking-like structures upon ICAM-1 engagement by anti-ICAM beads. Activated HUVECs were incubated with anti-ICAM beads for 15 minutes at 37ºC to engage ICAM-1 on endothelial cells (ECs), followed by washing and fixation. (A) Fluorescence micrographs were obtained at different planes along the z-axis (i to iv, where iv is closest to the plasma membrane), after staining anti-ICAM on the surface of beads using a FITC-labeled secondary antibody and ICAM-1 on the EC surface using a Texas Red-labeled antibody. Scale bar = 5 μm. (B) Scanning electron micrograph of an anti-ICAM bead being engulfed (black arrows) by an EC. Scale bar = 2.5 μm. (C) Fluorescence immunostaining of tetraspanin CD9 in ECs, at regions of binding of anti-ICAM beads. Left panel shows a micrograph showing CD9 enrichment as ring-like structures (white arrows). Scale bar = 10 μm. Right panel shows CD9 fluorescence intensity plot at the mid cross-section plane of anti-ICAM beads. Data represent mean and s.e.m. ($n \geq 100$ beads).

Then, using non-fluorescent beads to minimize optical interference while fluorescently labeling lipids of the plasma membrane, we observed that typical lipid raft-domain components such as cholesterol, sphingomyelin and ganglioside GM1 were enriched in areas of engulfment of anti-ICAM beads that mimic endothelial docking structures (ring-shaped fluorescent regions in Figure 9A). Semi-quantitative analysis (see Materials and Methods) revealed that the fluorescence intensity of the labeled lipids was increased by 1.6±0.04-fold, 3.1±0.1-fold, and 4.7±0.4-fold, for cholesterol, sphingomyelin and ganglioside GM1, respectively, in regions of bead engulfment by ICAM-1 engagement versus adjacent "background" areas (Fig. 10A). At the concentration used, neither Cdx treatment to chelate cholesterol (confirmed in Figures 9B and 10B, top panels) nor amiloride treatment to inhibit CAM-mediated pathway affected firm binding of anti-ICAM beads to ECs (compare phase-contrast pictures in Figures 9A, 9B, and 11 showing beads bound to ECs after several rounds of washes). However, both Cdx and amiloride decreased bead engulfment, as reflected by reduced ICAM-1 signal at the middle plane around beads (41.7% and 29.2% decrease, respectively; Figs 9B, 10B, and 11). These results correlate well with our findings showing that disruption of lipid domains and CAM-mediated pathway affect both WBC-EC pre-transmigration interactions and WBC TEM (Figs 5 and 7).

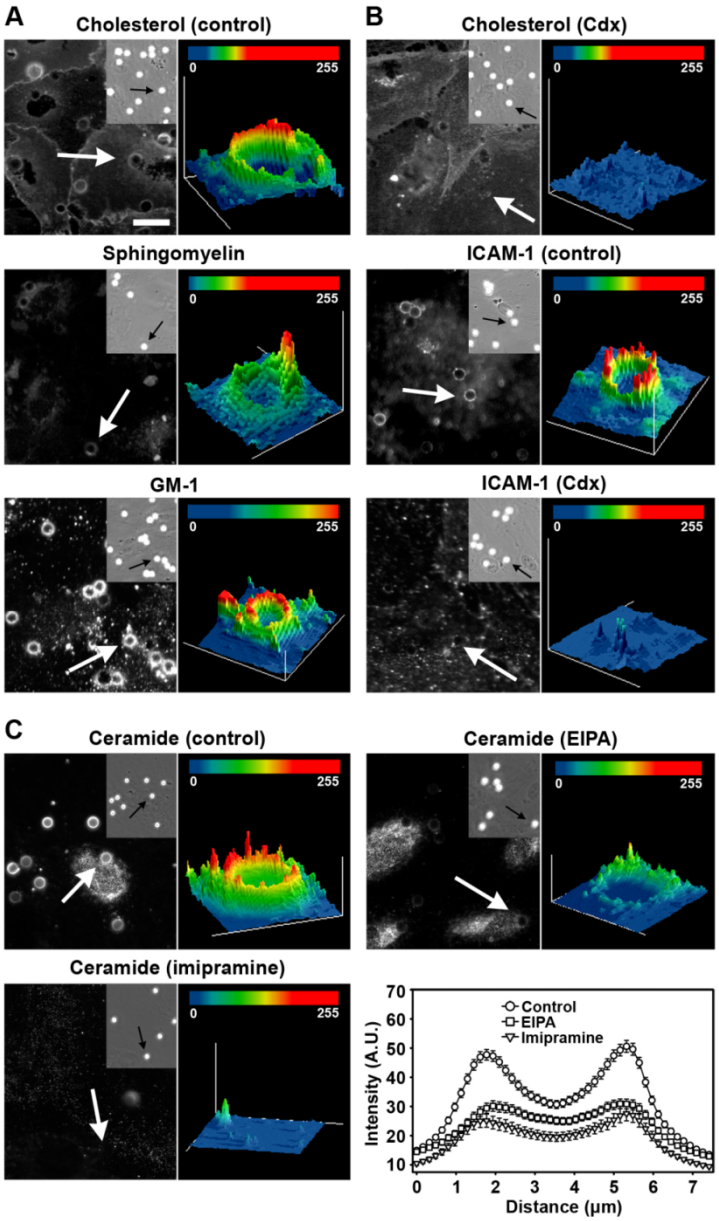

Figure 9. Recruitment of molecules at sites of endothelial ICAM-1 engagement by anti-ICAM beads. Activated HUVECs were incubated with anti-ICAM beads for 15 minutes at 37ºC to engage ICAM-1 on endothelial cells (ECs), followed by washing and fixation. (A) Cholesterol (top panel), sphingomyelin (middle panel) or ganglioside GM1 (bottom panel) were stained using fluorescent blue filipin, green BODIPY-sphingomyelin, or anti-GM1 and a Texas Red-labeled secondary antibody, respectively. (B) Effect of methyl-β-cyclodextrin (Cdx) on enrichment of cholesterol labeled with blue filipin (top panel) or ICAM-1 immunostained with a Texas Red-labeled antibody (middle and bottom panels) in regions of anti-ICAM bead binding. (C) Immunostaining of ceramide using a FITC-labeled antibody in regions of anti-ICAM-bead binding in control (top left panel), imipramine-treated (bottom left panel), and EIPA-treated (top right panel) cells. The bottom right panel shows ceramide fluorescence intensity plots at the mid cross-section plane of anti-ICAM beads bound to ECs under control (circles), imipramine (triangles), or EIPA (squares) conditions. In all cases, left sub-panels show fluorescence micrographs and phase-contrast insets of bound beads. Right sub-panels show pseudocolored fluorescence intensity reconstructions of molecules in the EC plasmalemma at areas of bound beads, which are indicated by arrows on their respective left sub-panels and insets. Scale bar = 20 μm. Data represent mean and s.e.m. ($n \geq 150$ beads).

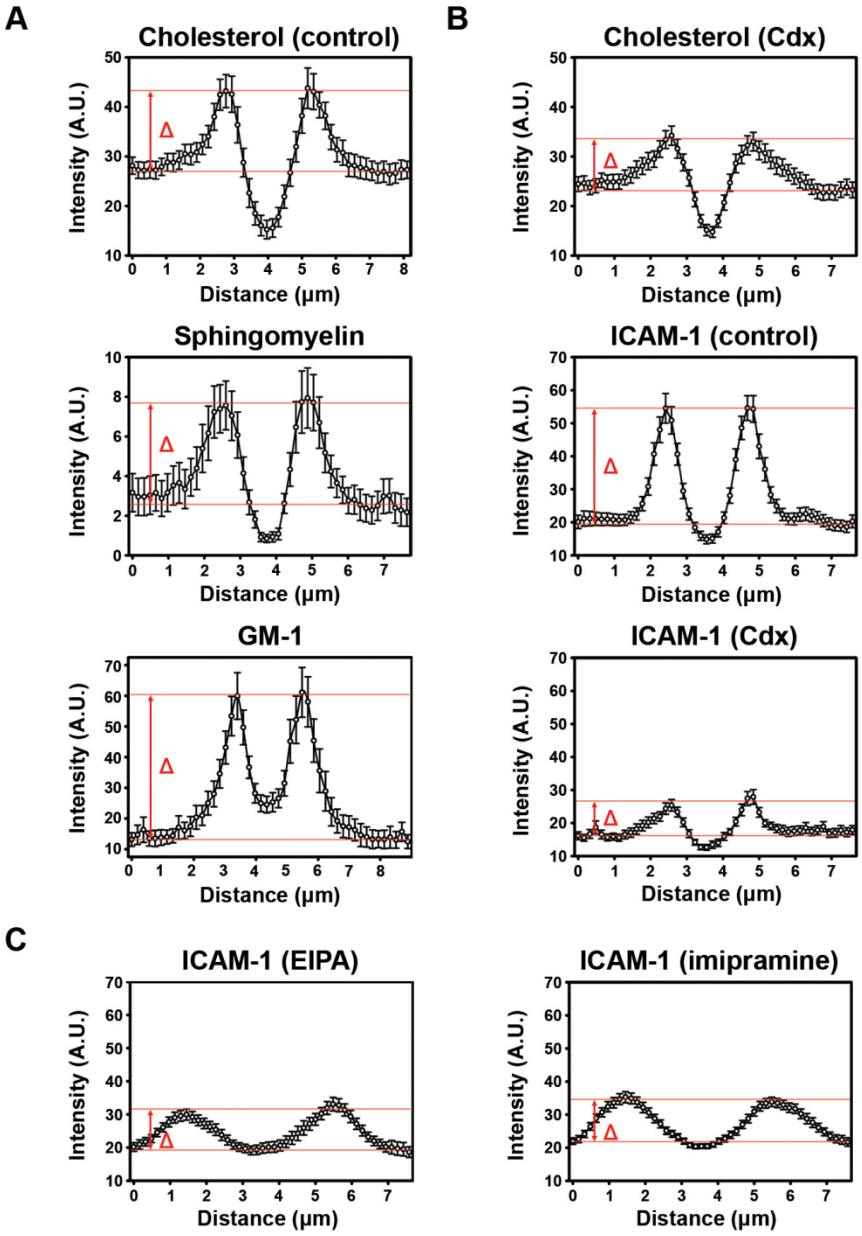

Figure 10. Quantification of enrichment of molecules at the endothelial plasmalemma in areas of ICAM-1 engagement by anti-ICAM beads. Activated HUVECs were incubated with anti-ICAM beads for 15 minutes at 37ºC to engage ICAM-1 on endothelial cells (ECs), followed by washing and fixation. (A) Cholesterol (upper panel), sphingomyelin (middle panel) or ganglioside GM1 (bottom panel), were stained using fluorescent blue filipin, green BODIPY-sphingomyelin, or anti-GM1 and a Texas Red-conjugated secondary antibody, respectively. (B) Effect of methyl-β-cyclodextrin (Cdx) on enrichment of cholesterol labeled with blue filipin (upper panel) or ICAM-1 immunostained with a Texas Red-labeled antibody (middle and bottom panels) in regions of anti-ICAM-bead binding. (C) Effect of EIPA and imipramine on ICAM-1 immunostained with a Texas Red-conjugated antibody in regions of anti-ICAM-bead binding. In all cases, graphs show fluorescence intensity plots at the mid cross-section plane of anti-ICAM beads bound on ECs, and enrichment of molecules in these engulfment areas compared to adjacent areas of the endothelial plasmalemma (Δ, which indicates fold increase). Data represent mean and s.e.m. (n ≥ 65 beads).

Furthermore, since hydrolysis of sphingomyelin into ceramide contributes to formation of large lipid domains, and this pathway is associated with modulation of the plasmalemma plasticity and cytoskeletal signaling[75-78], features required during leukocyte TEM, we tested for ceramide at regions of ICAM-1 engagement by anti-ICAM beads. As shown in Figure 9C, ceramide also increased over adjacent areas at these regions (3.5±0.01-fold), which was impaired by EIPA (35.6% decrease; Fig. 9C), an amiloride derivative that more specifically inhibits NHE1 involved in CAM-mediated endocytosis[29,71]. EIPA also reduced bead engulfment, causing reduced ICAM-1 signal around beads (42.7% decrease; Fig. 10C). This suggests for the first time that NHE1 may connect the CAM-mediated pathway to sphingomyelin/ceramide signaling.

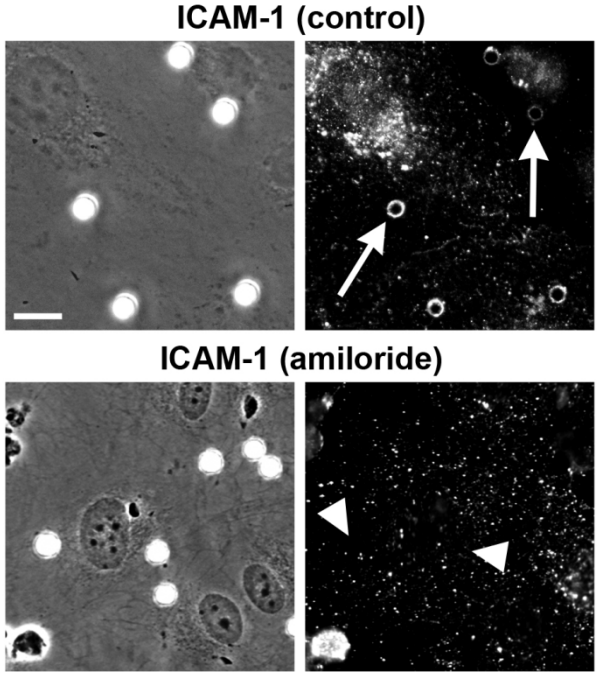

Figure 11. Effect of amiloride on the formation of ICAM-1-rich endothelial docking-like structures by anti-ICAM beads. Fluorescence micrographs show activated HUVECs incubated for 15 minutes at 37ºC with anti-ICAM beads to engage ICAM-1 on endothelial cells (ECs), under control conditions (top panel) or in the presence of amiloride (bottom panel). Cells were washed and fixed, ICAM-1 was immunostained using a Texas Red-labeled antibody, and samples were observed by phase-contrast (left panels) and fluorescence (right panels) microscopy. Presence or absence of bead engulfment is marked with arrows or arrowheads, respectively. Scale bar = 10 μm.

3.4. Recruitment of acid sphingomyelinase to endothelial docking-like structures. Contribution of the sphingomyelin/ceramide pathway to formation and/or maintenance of endothelial docking sites and structures at the interface between transmigrating leukocytes and ECs may require sphingomyelinase activity. Given that NHE1 provides acidification at the extracellular side of the plasmalemma[79], we inferred that ASM, a lysosomal enzyme that can be secreted[80], could be involved in ceramide generation at these regions. In accord with this, imipramine, a drug that inhibits ASM, impaired ceramide enrichment in areas of bead engulfment associated to ICAM-1 engagement (23.6% decrease; Fig. 9C), implicating for the first time ASM in ICAM-1-driven formation of endothelial docking-like structures.

In addition, immunofluorescence of ASM in ECs showed that, in absence of ICAM-1 engagement by anti-ICAM beads, most ASM located to vesicular compartments in the perinuclear region of cells (41.8±4.7 vesicles/cell), while few ASM-positive vesicles were found outside the perinuclear area (23.7±3.3 vesicles/cell; Fig. 12). ICAM-1 engagement by anti-ICAM beads lead to appearance of ASM-positive vesicles at the cell periphery (1.7-fold and 2.3-fold increase at 15 minutes and 30 minutes, respectively), and anti-ICAM bead engulfment areas became enriched in ASM (Fig. 13A). As negative controls for ICAM-1 specificity and optical artifacts, beads coated with antibodies to VCAM-1, also involved in leukocyte TEM, or M6PR, involved in clathrin-mediated transport of ASM[81], did not elicit ASM recruitment despite binding to ECs (Fig. 13A). Anti-M6PR beads induced recruitment neither of ICAM-1 nor NHE1, but recruited clathrin heavy chain (Fig. 14), validating this model. Importantly, areas of bead engulfment mediated by ICAM-1 engagement (Fig. 13B) revealed that ASM colocalized

well with both ICAM-1 and NHE1 (85.1±2.9% and 85.3±3.4% of total beads were positive for the two molecules, respectively). At high image magnification, ASM appeared to distribute within ICAM-1- and NHE1-lined vesicular structures (Fig. 13B, 16X panels).

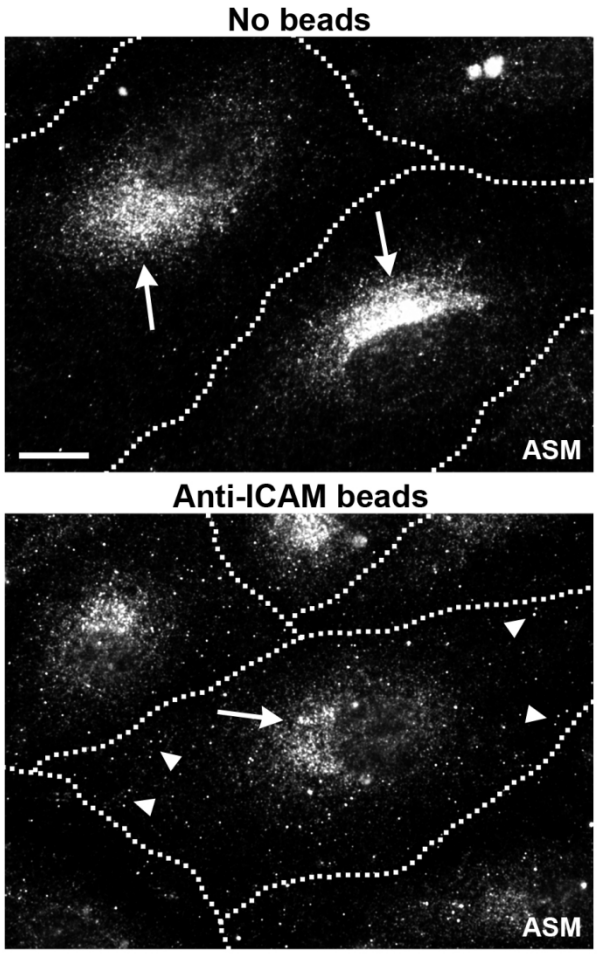

Figure 12. Intracellular redistribution of endothelial acid sphingomyelinase upon ICAM-1 engagement by anti-ICAM beads. Activated HUVECs were incubated in the absence (top panel) or presence (bottom panel) of anti-ICAM beads for 30 minutes at 37ºC. Cells were fixed and permeabilized, and ASM was stained with a Texas Red-labeled secondary antibody. Arrowheads mark ASM at the perinuclear region of cells. Arrows mark ASM at the cell periphery. Dashed lines mark the cell borders, as observed by phase contrast. Scale bar = 10 μm.

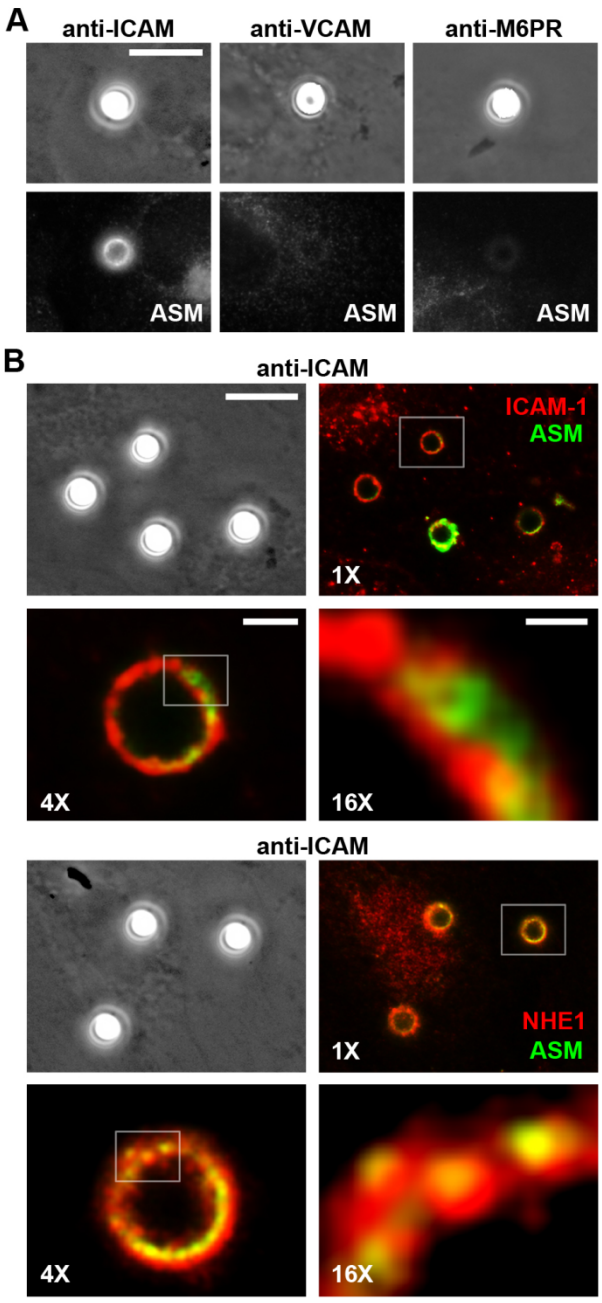

Figure 13. Plasmalemma distribution of endothelial acid sphingomyelinase upon ICAM-1 engagement by anti-ICAM beads. Activated HUVECs were incubated with anti-ICAM, anti-VCAM or anti-M6PR beads for 15 minutes at 37ºC to engage these molecules on endothelial cells (ECs), followed by washing and fixation. (A) Fluorescence immunostaining of ASM (bottom panels) in regions of respective bead binding (phase-contrast, top panels). Scale bar = 10 μm. (B) Fluorescence microscopy showing immunostaining of ASM (green), and ICAM-1 (red, top four panels) or NHE1 (red, bottom four panels). Boxes indicate the respective beads and bead regions selected for enlargement in 4X and 16X panels, as indicated. Scale bars = 10 μm in phase-contrast panel, 2 μm in 4X panel, and 0.5 μm in 16 X panel.

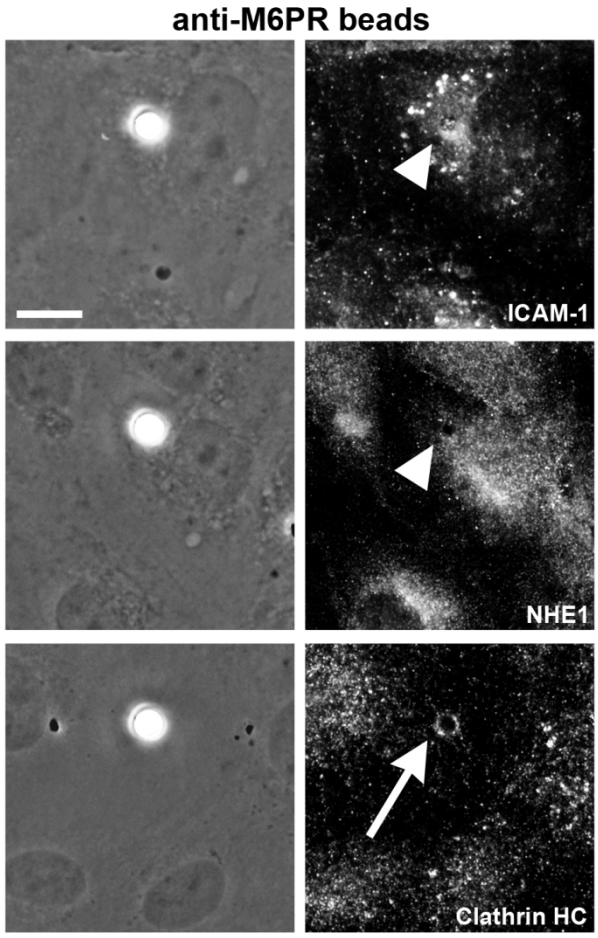

Figure 14. Recruitment of molecules at sites of anti-M6PR bead binding. Activated HUVECs were incubated with anti-mannose-6-phosphate receptor (M6PR) beads for 15 minutes at 37ºC to engage M6PR on endothelial cells (ECs), followed by washing and fixation. Phase contrast (left panels) and fluorescence micrographs (right panels) were obtained after immunostaining ICAM-1 (top), NHE1 (middle), or clathrin heavy chain (bottom) with Texas Red. Arrowheads indicate lack of enrichment of the corresponding marker around beads. Arrows indicate enrichment of the corresponding marker around beads. Scale bar = 10 μm.

3.5. Effect of impairing acid sphingomyelinase on CAM-mediated endocytosis and associated cytoskeletal rearrangement. Ceramide production by ASM at sites of ICAM-1 engagement where NHE1 may acidify the milieu could provide plasmalemma plasticity and likely activate cytoskeleton-associated signaling[75-78] required by endothelial docking-like structures involved in engulfment of micron-sized objects and pre-transmigratory structures at the interaction with leukocytes, to which we believe CAM-

mediated endocytosis may contribute. To explore this aspect, we tracked internalization of anti-ICAM beads by ECs using a microscopy technique extensively employed in our previous works, which differentially distinguishes surface-bound beads (accessible to a fluorescently-labeled secondary antibody that marks anti-ICAM on beads) versus beads residing within EC compartments (non-accessible to said secondary antibody)[29].

In agreement with our hypothesis, inhibition of ASM with imipramine and Na^+ depletion (to impair Na^+/H^+ transport and extracellular acidification) decreased endocytosis of anti-ICAM beads by ECs (from ~38% to 93% reduction; Table 2). This is similar to the previously observed inhibition of CAM-mediated endocytosis by affecting NHE1 with amiloride, and opposed to lack of an effect by treatment with filipin (~86% reduction versus ~7% increase, respectively; Table 2). ASM involvement was also confirmed in genetically modified models, to circumvent specificity concerns of pharmacological inhibitors. As shown in Table 2, using ECs isolated from wild-type versus $ASM^{-/-}$ mice, we observed that lack of ASM reduced endocytosis of anti-ICAM beads (75% reduction compared to ECs isolated from wild-type mice; Table 2).

Table 2. Inhibition of CAM-mediated endocytosis in the context of acid sphingomyelinase function.

	Internalization (%)
HUVECs	
Control	100.0±7.6
Amiloride	13.8±3.3**
Imipramine	61.9±6.7**
Na^+ depletion	7.4±2.5**
Filipin	107.2±1.5
MLECs	
Control	100.0±25.4
$ASM^{-/-}$	25.4±10.5*

Values are normalized to controls.
* is $P \leq 0.05$ and ** is $P \leq 0.001$.
$n \geq 10$ micrographs from 2 replicates.

This was further confirmed *in vivo* by injecting anti-ICAM beads intravenously in wild-type, caveolin-$1^{-/-}$ or $ASM^{-/-}$ mice, followed by isolation of lungs 3 h after injection and visualization by transmission electron microscopy. As in cell cultures, engulfment leading to endocytosis of anti-ICAM beads by ECs was inhibited in $ASM^{-/-}$ mice but not in caveolin-$1^{-/-}$ mice (12.2% and 92.8% of wild-type mice; Fig. 15). In $ASM^{-/-}$ mice, fewer membrane invaginations were detected in association with anti-ICAM beads (Fig. 15i,iv,vii), and the beads internalized in these mice were individually located within vesicles (Fig. 15ix), in contrast to large vesicular structures containing multiple beads observed in wild-type and caveolin-$1^{-/-}$ mice (Fig. 15iii,vi).

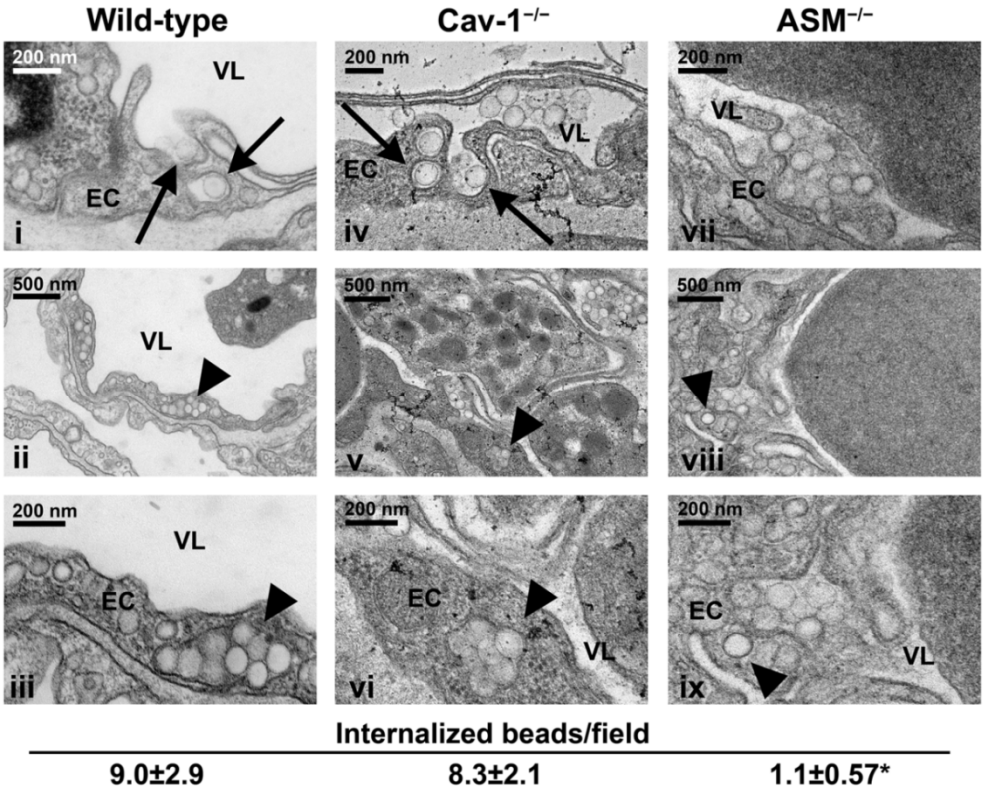

Figure 15. CAM-mediated endocytosis *in vivo*. Wild-type (i-iii), caveolin-$1^{-/-}$ (iv-vi), or $ASM^{-/-}$ (vii-ix) mice were injected intravenously under anesthesia with anti-ICAM beads and after 3 h lungs were isolated, perfused, and processed for transmission electron microscopy. Arrows indicate beads being internalized in endothelial invaginations. Arrowheads indicate beads fully internalized in intracellular vesicles. EC = endothelial cell, VL = (blood) vessel lumen. Scale bars = 200 nm or 500 nm, as indicated. The number of beads internalized within ECs was quantified from the micrographs. Data represent mean and s.e.m. ($n \geq 13$ micrographs). *, $P \leq 0.05$ by Student's t test.

Along with CAM-mediated endocytosis, imipramine treatment to inhibit ASM also disrupted formation of actin stress fibers that are induced by ICAM-1 engagement on ECs using anti-ICAM beads. In particular, formation of stress fibers within the cell body (versus cell edges) seemed most affected (Fig. 16A). This finding implies that ASM recruitment to sites of ICAM-1 engagement occurs prior to cytoskeletal rearrangement. Confirming this, inhibition of PKC, which has been reported to regulate formation of actin stress fibers by CAM-mediated endocytosis, did not affect ASM recruitment at ICAM-1 binding sites, but did inhibit uptake of anti-ICAM beads (Fig. 16B) and both these events were independent of PI3K signaling (Fig. 16B).

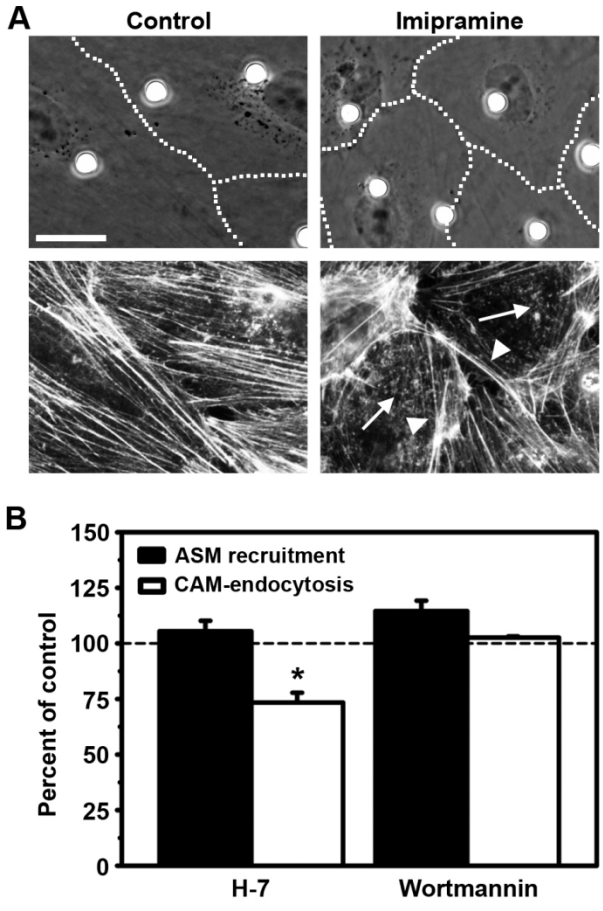

Figure 16. Acid sphingomyelinase and cytoskeleton-associated signaling upon ICAM-1 engagement. Activated HUVECs were incubated with anti-ICAM beads for 15 minutes (except for black bars in B, see below) at 37ºC to engage ICAM-1 on endothelial cells (ECs) under control conditions or in the presence of imipramine, H-7, or wortmannin, as indicated. (A) Top panels show phase-contrast micrographs of bound beads, with dashed lines indicating cell borders as seen through phase-contrast. Bottom panels show actin staining with Alexa Fluor 594-labeled phalloidin of control versus imipramine-treated cells. Arrows show disruption of actin stress fibers in the EC body. Arrowheads show actin stress fibers near cell edges. Scale bar = 20 μm. (B) Black bars: ASM was stained as in Figure 13 and enrichment was quantified by generating fluorescence intensity plots at the mid cross-section plane of anti-ICAM beads as in Figure 9. Data are normalized to control ($n \geq 75$ beads). White bars: Activated HUVECs were incubated with anti-ICAM beads for 1 hour at 37ºC to allow for internalization. Non-bound beads were washed, cells were fixed, and surface-bound beads were immunostained in Texas Red. Total amount of beads was quantified from phase-contrast images and surface-bound non-internalized beads were quantified by fluorescence microscopy to calculate the percent of internalized beads. Data represent mean and s.e.m. ($n \geq 20$ cells). *, $P \leq 0.01$ by Student's t test.

3.6. Acid sphingomyelinase in pre-transmigration interactions between leukocytes and endothelial cells. The results above, linking CAM-mediated endocytosis to ASM suggest that ASM may be involved in regulating leukocyte-EC interactions at pre-transmigratory sites. If this is the case, ASM must appear at such areas of leukocyte migration across ECs and its inhibition should affect said interactions. Confirming this, fluorescence microscopy revealed enrichment of ASM (immunostained in Texas Red, marked by arrows in Figure 17A) at the interface between ECs and sampling WBCs (stained with green calcein). This is similar to our observations of endothelial docking-like structures formed upon sole engagement of ICAM-1 by anti-ICAM beads (Fig. 13). Imipramine treatment to inhibit ASM led to a decrease in sampling WBCs (46.6±7.6% of control; Fig. 17B), without affecting WBC binding to ECs (108.0±18.6% of control). As shown for Cdx and amiloride in Figure 7, ASM inhibition with imipramine decreased the number of WBCs sampling the EC body below that of WBCs sampling the EC border (Fig. 17C). From the WBC population located within the EC body, there was a decrease in sampling WBCs and an increase in WBCs simply adhered (Fig. 17D). These results suggest that ASM activity linked to ICAM-1-engagement may be involved in the regulation of pre-transmigratory sites at the EC plasmalemma, and that this may be of particular relevance for transcellular TEM processes.

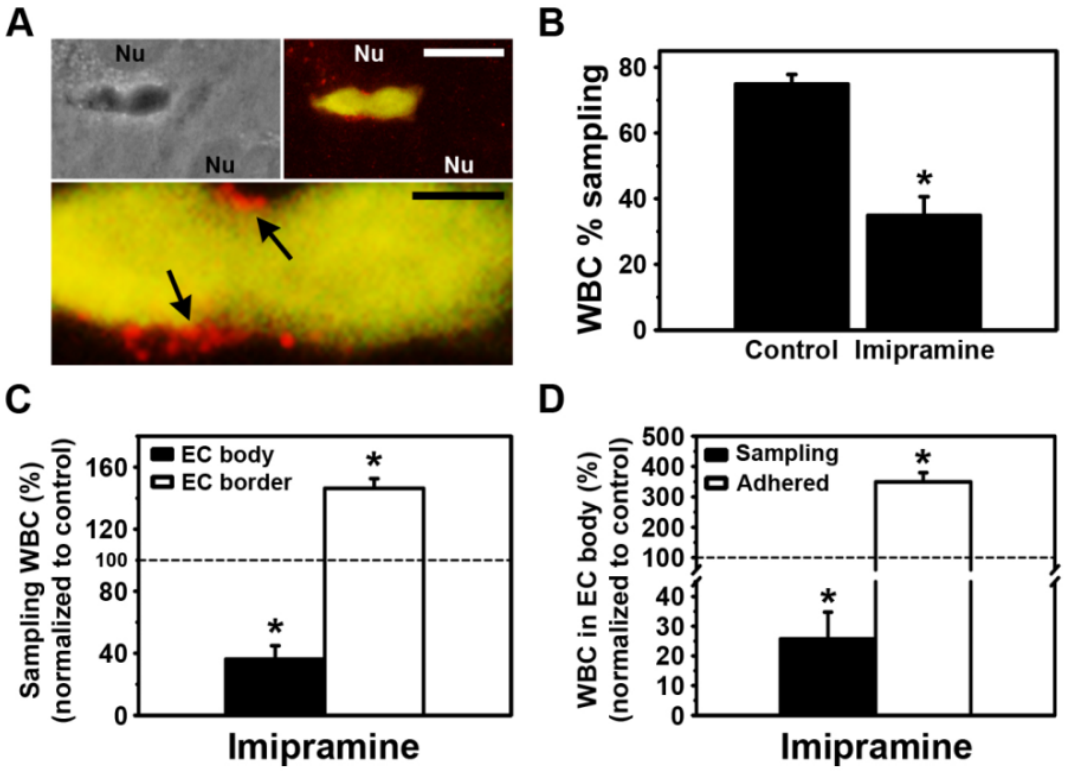

Figure 17. Acid sphingomyelinase enrichment at the interface between white blood cells and endothelial cells and its role in WBC sampling. Interaction of activated peripheral-blood lymphocytes (WBCs, pre-stained with green fluorescent calcein) with activated HUVECs growing on glass coverslips, determined after co-incubation for 30 minutes at 37ºC in control medium or medium containing imipramine, and analyzed by fluorescence microscopy as described for Figure 7. (A) Phase contrast (top left panel) and Texas Red immunostaining of ASM (top right and bottom panels) at the WBC-HUVEC interface in control conditions. ASM enrichment at these sites is marked by black arrows. Nu = nucleus. Scale bars = 10 μm in top right panel, and 2 μm in bottom panel. (B) Percent of sampling WBCs, calculated from WBCs firmly bound to HUVECs (black bars). (C) Spatial distribution of sampling WBCs, scored as occurring at either the EC body (black bar) or the EC border (white bar). (D) Fraction of sampling WBCs (black bar) versus simply adhered WBCs (white bar) within those located at the EC body. Data are normalized to control values (horizontal dashed lines), and represent mean and s.e.m. ($n \geq 100$ WBCs). *, $P \leq 0.01$ by Student's t test.

Chapter 4: Discussion

CAM-mediated endocytosis is an NHE1/dynamin-dependent, clathrin- and caveolae-independent endocytic pathway induced by engagement of ICAM-1 on ECs (e.g., by means of anti-ICAM conjugates and polymer beads)[29,66,71]. It results in massive cytoskeletal rearrangement with formation of actin stress fibers and endocytic vesicles between ~200 nm and several micrometers in diameter, which occurs without disruption of the EC junctions and seems involved in ICAM-1 recycling[29,66,71,82]. The results described in this work support a potential contribution of this pathway, along with sphingomyelin/ceramide signaling, to regulation of plasmalemma structures on ECs associated with leukocyte transmigration during inflammation.

It is known that, in addition to leukocytes[35,48,83,84], the endothelium plays an active role in defining the transmigration route (i.e., paracellular versus transcellular) during leukocyte TEM[19,48,49,55,56,85]. ECs extend dynamic actin-anchored ICAM-1-rich protrusions that engulf leukocytes (transmigratory cups or docking structures), providing tractive force for transmigration[19,48,55]. In the case of transcellular TEM, endothelial endocytic vesicles that form at these sites coalesce generating a transcellular pore through which leukocytes transmigrate[48,53]. The fact that ICAM-1, compared to other adhesion molecules, plays a key role in transcellular TEM[19,34,49,50,55] supports our findings that endocytic events induced by ICAM-1 engagement (CAM-mediated pathway) are involved, at least to some extent, in the regulation of this process.

During CAM-mediated endocytosis, ICAM-1 interacts with the Na^+/H^+ exchanger NHE1[29,71]. This exchanger, which is known to be involved in cytoskeletal rearrangement[86,87], acts as a crosslinker of actin filaments to the cytosolic domain of

ICAM-1[71]. The ion exchange activity of NHE1 also regulates the elasticity of the endothelial apical surface[88], in agreement with high permissibility of CAM-mediated endocytosis for engulfment and uptake of large micron-sized objects *in vitro* and *in vivo*[66]. Presumably, such deformability properties of CAM-mediated endocytosis would suitably adapt for formation of large endothelial docking structures, the wide range of sizes exhibited by the invasive podosomes and related structures that leukocytes extend into ECs during TEM, and possibly formation of transcellular pores observed in transcellular TEM[48,53].

Also in the context of CAM-mediated endocytosis and leukocyte TEM, diffusion of molecules in the plasmalemma must be temporarily reduced in areas of binding to ICAM-1, to permit formation of engagement and signaling platforms and to anchor the cytoskeleton, which has been recently observed[33]. The level of deformability required to engulf large objects and cells by endothelial docking structures progressing into transmigration pores must also relate to a particular lipid composition of the plasmalemma. Indeed, leukocyte TEM has been linked to cholesterol-, sphingomyelin-, and/or ganglioside-rich areas in lipid rafts and tetraspanin domains[49,57,74]. As shown in this work, such domains seem to be related also to the CAM-mediated pathway and are associated to induction of sphingomyelin/ceramide signaling upon ICAM-1 engagement at the EC plasmalemma.

The enrichment in ceramide at endothelial docking-like structures induced by ICAM-1 engagement is likely to impact the molecular and biophysical features of these areas of the plasma membrane. As observed in other systems, ceramide confers particular properties to the membrane environment depending on the ratio of raft components[89],

e.g., it can promote the formation of large lipid domains[76,77] or displace lipid domain constituents to affect membrane function[75]. Ceramide production by ASM at the outer leaflet of the plasma membrane modifies its curvature and results in vesiculization[77,78,90], as well as cytoskeletal rearrangement[75,91], supporting similar observations in this work. These events downstream of the sphingomyelin/ceramide pathway could contribute to formation of large micron-sized vesicles, as observed in CAM-mediated endocytosis (Table 2)[29,66]. In addition, ceramide production by (acid) sphingomyelinase is known to be associated with vesicular fusion[92,93], which is in accord with our results showing the accumulation of several anti-ICAM beads within the same intracellular compartment in wild-type, but not $ASM^{-/-}$ mouse endothelium (Fig. 15).

Supporting the link between CAM-mediated endocytosis, ASM, and the formation of dynamic, fusing vesicles, unpublished work by other members of our group shows that ICAM-1 multivalent engagement using streptavidin-linked biotinylated anti-ICAM induces the formation of structures that resemble transcellular pores (Fig. 18). This is seen when anti-ICAM present on the cell surface versus internalized within endocytic vesicles is differentially immunostained before and after cell permeabilization using secondary antibodies conjugated to Texas Red or green FITC, respectively. In certain instances, regions of the endothelial membrane show internal, but not surface staining (Fig. 18A), indicating localized regions of endocytosis. Here, anti-ICAM-positive vesicles resulting from such endocytosis (~200-300 nm diameter; white arrowhead in Figure 18A) appear to be all grouped in bundles forming large structures (~10 μm diameter; arrows in Figure 18A). Numerous vesicles within these platforms appear to

fuse into larger vesicles (black arrowhead in Figure 18A), which resemble the preliminary steps into formation of a transcellular pore[53].

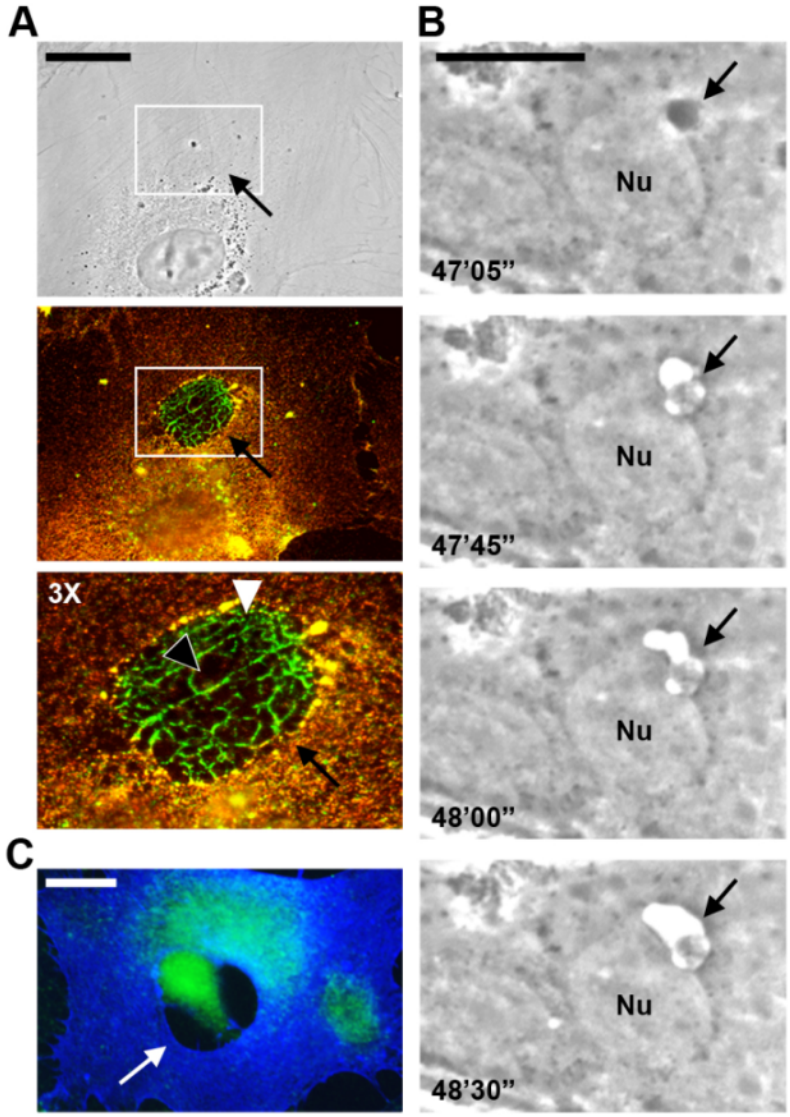

Figure 18. Induction of transcellular pore-like structures by ICAM-1 engagement. Activated HUVECs were incubated in the presence of anti-ICAM biotin-streptavidin conjugate (A), anti-ICAM beads (B), or green calcein-stained peripheral-blood lymphocytes (WBCs, C). (A) ICAM-1 double-stained on endothelial cells (ECs) with a Texas Red-labeled secondary antibody prior to permeabilization (cell surface), and a FITC-labeled secondary antibody post-permeabilization (internalized). Top panel shows phase contrast, where box indicates the location of a transcellular pore-like structure (black arrows) observed by fluorescence microscopy (middle panel). White arrowhead shows vesicles of 200-300 nm in diameter. Black arrowhead shows larger micrometer-size vesicles resulting from fusion. (B) Individual frames obtained from time-lapse phase-contrast microscopy (time is indicated in minutes (') and seconds ('')) showing formation of a transcellular pore-like structure underneath a bead bound to cell surface close to the nuclear region. Black arrows mark the original position of the anti-ICAM bead. (C) Green calcein-stained WBC found transmigrating through a transcellular pore (white arrow) formed on an EC whose surface was immunostained in blue with anti-ICAM. Nu = Nucleus. Scale bars = 10 μm.

Supporting these notions, dynamic time-lapse imaging using phase-contrast as shown in Figure 18B, allows to observe the sequential formation of a pore-like structure underneath a bound anti-ICAM bead, with the particle disappearing from the focal plane into the opening (Fig. 18B). This opening closely resembles genuine transmigration pores that form across ECs at sites of transcellular TEM of WBCs (Fig. 18C), suggesting that CAM-mediated pathway may contribute to this process.

Of note, such coalescence of CAM-derived vesicles into pore-like structures is difficult to track in time. The appearance of these structures often occurs concomitantly in most ECs in a given sample, yet this occurs at different time points (between 15 minutes and 1 hour tested) in independent experiments. This emphasizes the highly dynamic and transient nature of these events, which are likely to be subject to additional regulatory elements in more physiological conditions involving multiple leukocyte-EC interactions, perhaps also in concert with caveolar pathways. In any case, formation of transcellular pore-like structures from vesicles induced via CAM-mediated endocytosis is in agreement with our findings showing that this pathway operates through the sphingomyelin/ceramide pathway and may contribute to the overall process of transcellular TEM.

Also consistent with our findings, ECs constitutively secrete ASM, whose activity increases upon exposure to certain inflammatory cytokines[80], making ASM catalysis available at the plasmalemma. As found in this work, ICAM-1 engagement at the EC surface leads to ASM redistribution from perinuclear to non-perinuclear areas in ECs, accompanied by enrichment of this enzyme in regions of ICAM-1 engagement by anti-ICAM beads and WBCs (Figs 14, 17). It is known that lysosomes carrying ASM can be

exocytosed[90], a possible mechanistic explanation for the redistribution and presence of this enzyme at the plasmalemma in our study. Secretion of lysosomal ASM is mediated by increase in intracellular Ca^{2+} (ref. 94), a phenomenon also known to be involved in CAM-mediated endocytosis upon ICAM-1 engagement[71], additionally associated to leukocyte interaction with ECs[61].

Ceramide production by sphingomyelinases has also been tied to the inflammatory response under a variety of scenarios, including increased rolling and binding of leukocytes to brain endothelium[95]. Other work indicates that leukocyte influx into alveolar space is decreased in $ASM^{-/-}$ mice[96], and metabolic imbalances causing high levels of ceramide can lead to higher leukocyte levels in tissue[97]. Our data showing redistribution of ASM to endothelial docking-like structures and the interface between WBCs and ECs, along with enrichment of ceramide in these regions, are consistent with this literature.

Given that ICAM-1 interacts with NHE1 upon ICAM-1 engagement[71], and due to the directionality of NHE1 ion exchange (Na^+ influx / H^+ efflux)[79,86], it is expected that ion transport activity of NHE1 will locally acidify ICAM-1 engagement regions, creating a confined acidic microenvironment. A similar function of NHE1 has been shown in the context of certain pH-sensitive enzymes[79]. Particularly, inhibition of NHE1 with cariporide ameliorates the cisplatin-induced ceramide generation by ASM[98]. Secreted ASM, whose pK_a is acidic[80], should only be able to efficiently hydrolyze sphingomyelin into ceramide at NHE1-enriched, ICAM-1 engagement regions. This provides a suitable explanation on how an acidic enzyme can carry activity at the otherwise neutral

extracellular environment and may also contribute to understanding the means by which ECs regulate ceramide production with spatial precision.

Altogether, the data obtained in this work suggest a model (Fig. 19) by which engagement of ICAM-1 in lipid domains enriched in sphingomyelin induces secretion of ASM from intracellular compartments to these areas of the endothelial plasma membrane. At these sites, engaged ICAM-1 forms a complex with NHE1, which results in local acidification, sphingomyelin hydrolysis by secreted ASM, and local production of ceramide. This signal leads to actin polymerization and cytoskeleton remodeling, stabilizes the engagement platform by restricting molecular diffusion and providing cytoskeletal anchorage, regulates membrane deformability, and favors dynamic formation of CAM-mediated endocytic vesicles, which occurs at sites of leukocyte-podosome sampling in search from sites suitable for transcellular TEM. Finally, vesicular fusion mediated through sphingomyelin/ceramide signaling at this interface contributes to transmigration pores.

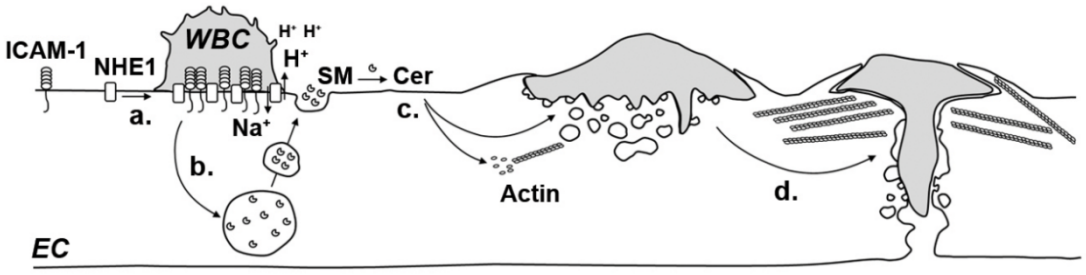

Figure 19. Model for the contribution of CAM-mediated endocytosis and the sphingomyelin/ceramide pathway to leukocyte transcellular transmigration. (a.) Binding of leukocytes to ICAM-1 located at cholesterol and sphingomyelin- (SM)-rich areas of the EC plasmalemma recruits NHE1 to binding sites and (b.) serves as a signal for redistribution of ASM from intracellular compartments to the EC surface. H+ extrusion by NHE1 at sites of ICAM-1 engagement creates a pH microenvironment optimal for ASM activity, where SM is hydrolyzed to ceramide (Cer). (c.) Ceramide production induces the rearrangement of the actin cytoskeleton and favors negative curvature of the membrane, resulting in formation of endothelial docking structures and endocytic vesicles at these sites. (d.) Ceramide-rich vesicles are prompt to vesicular fusion, which contributes to formation of a transcellular pore during leukocyte TEM.

Chapter 5: Conclusions and future directions

In this study, we found that ASM is involved in CAM-mediated endocytosis, and this pathway contributes to leukocyte transmigration, likely through the transcellular route by formation of endothelial docking structures and transcellular pores. Until recent years, the events regulating the route of leukocyte TEM (transcellular versus paracellular) have been difficult to elucidate. Our findings will be further tested in order to confirm that CAM-mediated endocytosis contributes particularly to leukocyte transcellular migration. This will involve the use a larger array of tools such as knockout and knockdown leukocytes and ECs, along anti-ICAM beads of different sizes and targeting different epitopes of ICAM-1, and animal models. As a key component of the inflammatory response, leukocyte TEM is associated with multiple immune diseases. For instance, paracellular migration, which involves the disassembly of cell-cell junctions[99,100], may lead, under pathological conditions, to excessive vascular permeability and leakage of plasma into tissue[101,102]. Potentiation of the transcellular route might allow for therapeutic intervention during pathological states or conditions where this is the case. Further, it has been recently shown that leukocytes can migrate transcellularly across fibroblasts[103]. Thus, it will be interesting to extend studies on the contribution of CAM-mediated endocytosis to transcellular migration across cell types other than ECs, and determine if there exist any physiological implications to these activities. Indeed, we have seen CAM-mediated endocytosis occur in cell types other than ECs.

The found contribution by ASM to CAM-mediated endocytosis in this work reinforces the emerging role of this enzyme during signaling and inflammatory events, which should be further studied in order to understand how the multiple functions ascribed to

ASM[80,104] are regulated. Ceramide production at the plasma membrane elicits diverse signaling events[75,80,91,105-107], and has been linked to the entry of pathogens into cells[108-110]. Vesicle formation by ceramide appears to be independent of other cellular factors[78], and thus, it might be possible to use sphingomyelinases to drive endocytosis of objects under a variety of scenarios. This might constitute a new tool in the modulation of controlled therapeutic delivery into cells, and future work in our lab will study the possibility of using ceramide to enhance the entry of large objects into cells, besides those that elicit CAM-mediated uptake.

However, the role of ceramide during CAM-mediated endocytosis goes beyond the formation of vesicles, as our findings suggest that ceramide is also involved in formation of docking structures, and rearrangement of the actin cytoskeleton into stress fibers. It will be interesting to understand the mechanisms through which ceramide achieves these outcomes during leukocyte transmigration and other phenomena that depend on endocytosis and cytoskeletal rearrangement. For instance, certain groups have hypothesized that multivalent engagement of ICAM-1 induces formation of actin stress fibers by displacement of ezrin/moesin from the cytosolic tail of ICAM-1, followed by recruitment of cortactin[111]. Indeed, ceramide production at the plasma membrane causes dephosphorylation of ezrin and its displacement to the cytosol[75]. Confirming and elucidating mechanistic steps such as this one will be crucial for full understanding of the links between the sphingomyelin/ceramide pathway, CAM-mediated endocytosis, and leukocyte TEM.

Finally, other natural ligands of ICAM-1 include fibrin, rhinovirus, poliovirus, HIV, some bacteria[112], and *Plasmodium falciparum*-infected erythrocytes during malarial

infection[113]. Future work should address potential role of CAM-mediated endocytosis, along with newfound player ASM, in the uptake of these molecules and organisms by cells, transport into tissue, and possible development of therapeutic interventions.

Literature cited

1. Muro S. ICAM-1 and VCAM-1. In: Aird WC, ed. Endothelial Biomedicine. Cambridge University Press. Ney York, NY. 2007:1058-1070.
2. Dustin ML, Rothlein R, Bhan AK, Dinarello CA, Springer TA. Induction by IL 1 and interferon-γ: tissue distribution, biochemistry, and function of a natural adherence molecule (ICAM-1). The Journal of Immunology. 1986;137:245-254.
3. Myers CL, Wertheimer SJ, Schembri-King J, Parks T, Wallace RW. Induction of ICAM-1 by TNF-alpha, IL-1 beta, and LPS in human endothelial cells after downregulation of PKC. American Journal of Physiology. 1992;263:C767-772.
4. Kirchhausen T, Staunton DE, Springer TA. Location of the domains of ICAM-1 by immunolabeling and single-molecule electron microscopy. Journal of Leukocyte Biology. 1993;53:342-346.
5. Yang Y, Jun C-D, Liu J-H, et al. Structural basis for dimerization of ICAM-1 on the cell surface. Molecular Cell. 2004;14:269-276.
6. Diamond MS, Staunton DE, de Fougerolles AR, et al. ICAM-1 (CD54): a counter-receptor for Mac-1 (CD11b/CD18). The Journal of Cell Biology. 1990;111:3129-3139.
7. Staunton DE, Dustin ML, Erickson HP, Springer TA. The arrangement of the immunoglobulin-like domains of ICAM-1 and the binding sites for LFA-1 and rhinovirus. Cell. 1990;61:243-254.
8. Staunton DE, Marlin SD, Stratowa C, Dustin ML, Springer TA. Primary structure of ICAM-1 demonstrates interaction between members of the immunoglobulin and integrin supergene families. Cell. 1988;52:925-933.

9. Pluskota E, Chen Y, D'Souza SE. Src homology domain 2-containing tyrosine phosphatase 2 associates with intercellular adhesion molecule 1 to regulate cell survival. The Journal of Biological Chemistry. 2000;275:30029-30036.

10. Pluskota E, D'Souza SE. Fibrinogen interactions with ICAM-1 (CD54) regulate endothelial cell survival. European Journal of Biochemistry. 2000;267:4693-4704.

11. Carpén O, Pallai P, Staunton DE, Springer TA. Association of intercellular adhesion molecule-1 (ICAM-1) with actin-containing cytoskeleton and α-actinin. The Journal of Cell Biology. 1992;118:1223-1234.

12. Federici C, Camoin L, Hattab M, Strosberg AD, Couraud PO. Association of the cytoplasmic domain of intercellular-adhesion molecule-1 with glyceraldehyde-3-phosphate dehydrogenase and β-tubulin. European Journal of Biochemistry. 1996;238:173-180.

13. Sans E, Delachanal E, Duperray A. Analysis of the roles of ICAM-1 in neutrophil transmigration using a reconstituted mammalian cell expression model: implication of ICAM-1 cytoplasmic domain and Rho-dependent signaling pathway. The Journal of Immunololy. 2001;166:544-551.

14. Pattillo CB, Pardue S, Shen X, et al. ICAM-1 cytoplasmic tail regulates endothelial glutathione synthesis through a NOX4/PI3-kinase-dependent pathway. Free Radical Biololgy & Medicine. 2010;49:1119-1128.

15. Greenwood J, Amos CL, Walters CE, et al. Intracellular domain of brain endothelial intercellular adhesion molecule-1 is essential for T lymphocyte-mediated signaling and migration. The Journal of Immunology. 2003;171:2099-2108.

16. Heiska L, Alfthan K, Grönholm M, Vilja P, Vaheri A, Carpén O. Association of ezrin with intercellular adhesion molecule-1 and -2 (ICAM-1 and ICAM-2). Regulation by phosphatidylinositol 4, 5-bisphosphate. The Journal of Biological Chemistry. 1998;273:21893-21900.

17. Wójciak-Stothard B, Williams L, Ridley AJ. Monocyte adhesion and spreading on human endothelial cells is dependent on Rho-regulated receptor clustering. The Journal of Cell Biology. 1999;145:1293-1307.

18. Thompson PW, Randi AM, Ridley AJ. Intercellular adhesion molecule (ICAM)-1, but not ICAM-2, activates RhoA and stimulates c-fos and rhoA transcription in endothelial cells. The Journal of Immunology. 2002;169:1007-1013.

19. Oh H-M, Lee S, Na B-R, et al. RKIKK motif in the intracellular domain is critical for spatial and dynamic organization of ICAM-1: functional implication for the leukocyte adhesion and transmigration. Molecular Biology of the Cell. 2007;18:2322-2335.

20. Etienne S, Adamson P, Greenwood J, Strosberg AD, Cazaubon S, Couraud PO. ICAM-1 signaling pathways associated with Rho activation in microvascular brain endothelial cells. The Journal of Immunology. 1998;161:5755-5761.

21. Holland J, Owens T. Signaling through intercellular adhesion molecule 1 (ICAM-1) in a B cell lymphoma line. The activation of Lyn tyrosine kinase and the mitogen-activated protein kinase pathway. The Journal of Biological Chemistry. 1997;272:9108-9112.

22. Durieu-Trautmann O, Chaverot N, Cazaubon S, Strosberg AD, Couraud PO. Intercellular adhesion molecule 1 activation induces tyrosine phosphorylation of

the cytoskeleton-associated protein cortactin in brain microvessel endothelial cells. The Journal of Biological Chemistry. 1994;269:12536-12540.

23. Wang Q, Pfeiffer GR, Gaarde WA. Activation of SRC tyrosine kinases in response to ICAM-1 ligation in pulmonary microvascular endothelial cells. The Journal of Biological Chemistry. 2003;278:47731-47743.

24. Adamson P, Etienne S, Couraud PO, Calder V, Greenwood J. Lymphocyte migration through brain endothelial cell monolayers involves signaling through endothelial ICAM-1 via a rho-dependent pathway. The Journal of Immunology. 1999;162:2964-2973.

25. Etienne-Manneville S, Manneville JB, Adamson P, Wilbourn B, Greenwood J, Couraud PO. ICAM-1-coupled cytoskeletal rearrangements and transendothelial lymphocyte migration involve intracellular calcium signaling in brain endothelial cell lines. The Journal of Immunology. 2000;165:3375-3383.

26. Wang Q, Doerschuk CM. The p38 mitogen-activated protein kinase mediates cytoskeletal remodeling in pulmonary microvascular endothelial cells upon intracellular adhesion molecule-1 ligation. The Journal of Immunology. 2001;166:6877-6884.

27. Wang Q, Yerukhimovich M, Gaarde WA, Popoff IJ, Doerschuk CM. MKK3 and -6-dependent activation of p38α MAP kinase is required for cytoskeletal changes in pulmonary microvascular endothelial cells induced by ICAM-1 ligation. American Journal of Physiology, Lung Cell Molecular Physiology. 2005;288:L359-369.

28. Amos C, Romero IA, Schültze C, et al. Cross-linking of brain endothelial intercellular adhesion molecule (ICAM)-1 induces association of ICAM-1 with detergent-insoluble cytoskeletal fraction. Arteriosclerosis, Thrombosis, and Vascular Biology. 2001;21:810-816.

29. Muro S, Wiewrodt R, Thomas A, et al. A novel endocytic pathway induced by clustering endothelial ICAM-1 or PECAM-1. Journal of Cell Science. 2003;116:1599-1609.

30. Wang Q, Chiang ET, Lim M, et al. Changes in the biomechanical properties of neutrophils and endothelial cells during adhesion. Blood. 2001;97:660-668.

31. Wang Q, Doerschuk CM. Neutrophil-induced changes in the biomechanical properties of endothelial cells: roles of ICAM-1 and reactive oxygen species. The Journal of Immunology. 2000;164:6487-6494.

32. Wittchen ES. Endothelial signaling in paracellular and transcellular leukocyte transmigration. Frontiers in Bioscience. 2009;14:2522-2545.

33. van Buul JD, van Rijssel J, van Alphen FPJ, et al. Inside-out regulation of ICAM-1 dynamics in TNF-α-activated endothelium. PLoS ONE. 2010;5:e11336.

34. Ley K, Laudanna C, Cybulsky MI, Nourshargh S. Getting to the site of inflammation: the leukocyte adhesion cascade updated. Nature Reviews Immunology. 2007;7:678-689.

35. Nourshargh S, Hordijk PL, Sixt M. Breaching multiple barriers: leukocyte motility through venular walls and the interstitium. Nature Reviews Molecular Cell Biology. 2010;11:366-378.

36. Engelhardt B, Wolburg H. Mini-review: Transendothelial migration of leukocytes: through the front door or around the side of the house? European Journal of Immunology. 2004;34:2955-2963.

37. Ley K, Bullard DC, Arbonés ML, et al. Sequential contribution of L- and P-selectin to leukocyte rolling *in vivo*. The Journal of Experimental Medicine. 1995;181:669-675.

38. Zarbock A, Abram CL, Hundt M, Altman A, Lowell CA, Ley K. PSGL-1 engagement by E-selectin signals through Src kinase Fgr and ITAM adapters DAP12 and FcR gamma to induce slow leukocyte rolling. The Journal of Experimental Medicine. 2008;205:2339-2347.

39. Kunkel EJ, Ley K. Distinct phenotype of E-selectin-deficient mice. E-selectin is required for slow leukocyte rolling in vivo. Circ Res. 1996;79:1196-1204.

40. Dunne JL, Ballantyne CM, Beaudet AL, Ley K. Control of leukocyte rolling velocity in TNF-α-induced inflammation by LFA-1 and Mac-1. Blood. 2002;99:336-341.

41. Sigal A, Bleijs DA, Grabovsky V, et al. The LFA-1 integrin supports rolling adhesions on ICAM-1 under physiological shear flow in a permissive cellular environment. The Journal of Immunology. 2000;165:442-452.

42. Salas A, Shimaoka M, Chen S, Carman CV, Springer T. Transition from rolling to firm adhesion is regulated by the conformation of the I domain of the integrin lymphocyte function-associated antigen-1. The Journal of Biological Chemistry. 2002;277:50255-50262.

43. Alon R, Kassner PD, Carr MW, Finger EB, Hemler ME, Springer TA. The integrin VLA-4 supports tethering and rolling in flow on VCAM-1. The Journal of Cell Biology. 1995;128:1243-1253.

44. Marlin SD, Springer TA. Purified intercellular adhesion molecule-1 (ICAM-1) is a ligand for lymphocyte function-associated antigen 1 (LFA-1). Cell. 1987;51:813-819.

45. Elices MJ, Osborn L, Takada Y, et al. VCAM-1 on activated endothelium interacts with the leukocyte integrin VLA-4 at a site distinct from the VLA-4/fibronectin binding site. Cell. 1990;60:577-584.

46. Dejana E. Endothelial cell-cell junctions: happy together. Nature Reviews Molecular Cell Biology. 2004;5:261-270.

47. Carman CV. Mechanisms for transcellular diapedesis: probing and pathfinding by 'invadosome-like protrusions'. Journal of Cell Science. 2009;122:3025-3035.

48. Carman CV, Springer TA. A transmigratory cup in leukocyte diapedesis both through individual vascular endothelial cells and between them. The Journal of Cell Biology. 2004;167:377-388.

49. Millán J, Hewlett L, Glyn M, Toomre D, Clark P, Ridley AJ. Lymphocyte transcellular migration occurs through recruitment of endothelial ICAM-1 to caveola- and F-actin-rich domains. Nature Cell Biology. 2006;8:113-123.

50. Yang L, Froio RM, Sciuto TE, Dvorak AM, Alon R, Luscinskas FW. ICAM-1 regulates neutrophil adhesion and transcellular migration of TNF-α-activated vascular endothelium under flow. Blood. 2005;106:584-592.

51. Cinamon G, Grabovsky V, Winter E, et al. Novel chemokine functions in lymphocyte migration through vascular endothelium under shear flow. Journal of Leukocyte Biology. 2001;69:860-866.

52. Luu NT, Rainger GE, Nash GB. Kinetics of the different steps during neutrophil migration through cultured endothelial monolayers treated with tumour necrosis factor-α. Journal of Vascular Research. 1999;36:477-485.

53. Carman CV, Sage PT, Sciuto TE, et al. Transcellular diapedesis is initiated by invasive podosomes. Immunity. 2007;26:784-797.

54. Carman CV, Jun C-D, Salas A, Springer TA. Endothelial cells proactively form microvilli-like membrane projections upon intercellular adhesion molecule 1 engagement of leukocyte LFA-1. The Journal of Immunology. 2003;171:6135-6144.

55. Barreiro O, Yanez-Mo M, Serrador JM, et al. Dynamic interaction of VCAM-1 and ICAM-1 with moesin and ezrin in a novel endothelial docking structure for adherent leukocytes. The Journal of Cell Biology. 2002;157:1233-1245.

56. van Buul JD, Allingham MJ, Samson T, et al. RhoG regulates endothelial apical cup assembly downstream from ICAM1 engagement and is involved in leukocyte trans-endothelial migration. The Journal of Cell Biology. 2007;178:1279-1293.

57. Tilghman RW, Hoover RL. E-selectin and ICAM-1 are incorporated into detergent-insoluble membrane domains following clustering in endothelial cells. FEBS Letters. 2002;525:83-87.

58. Mamdouh Z, Mikhailov A, Muller WA. Transcellular migration of leukocytes is mediated by the endothelial lateral border recycling compartment. Journal of Experimental Medicine. 2009;206:2795-2808.

59. Smith CW, Marlin SD, Rothlein R, Toman C, Anderson DC. Cooperative interactions of LFA-1 and Mac-1 with intercellular adhesion molecule-1 in facilitating adherence and transendothelial migration of human neutrophils *in vitro*. The Journal of Clinical Investigation. 1989;83:2008-2017.

60. Lawson C, Wolf S. ICAM-1 signaling in endothelial cells. Pharmacological Reports. 2009;61:22-32.

61. Huang AJ, Manning JE, Bandak TM, Ratau MC, Hanser KR, Silverstein SC. Endothelial cell cytosolic free calcium regulates neutrophil migration across monolayers of endothelial cells. The Journal of Cell Biology. 1993;120:1371-1380.

62. Yang L, Kowalski JR, Zhan X, Thomas SM, Luscinskas FW. Endothelial cell cortactin phosphorylation by Src contributes to polymorphonuclear leukocyte transmigration in vitro. Circulation Research. 2006;98:394-402.

63. Muro S, Cui X, Gajewski C, Murciano J-C, Muzykantov VR, Koval M. Slow intracellular trafficking of catalase nanoparticles targeted to ICAM-1 protects endothelial cells from oxidative stress. American Journal of Physiology, Cell Physiology. 2003;285:C1339-1347.

64. Muro S, Gajewski C, Koval M, Muzykantov VR. ICAM-1 recycling in endothelial cells: a novel pathway for sustained intracellular delivery and prolonged effects of drugs. Blood. 2005;105:650-658.

65. Ghaffarian R. Study of ICAM-1-targeted nanocarriers as a strategy for drug delivery across the intestinal epithelium. Biology B.S. Thesis. College Park, MD: University of Maryland College Park; 2010:36.

66. Muro S, Garnacho C, Champion JA, et al. Control of endothelial targeting and intracellular delivery of therapeutic enzymes by modulating the size and shape of ICAM-1-targeted carriers. Molecular Therapy. 2008;16:1450-1458.

67. Caron E, Hall A. Phagocytosis. In: Marsh M, ed. Endocytosis. Oxford: Oxford University Press; 2001:58-77.

68. Horinouchi K, Erlich S, Perl DP, et al. Acid sphingomyelinase deficient mice: a model of types A and B Niemann-Pick disease. Nature Genetics. 1995;10:288-293.

69. Dong QG, Bernasconi S, Lostaglio S, et al. A general strategy for isolation of endothelial cells from murine tissues. Characterization of two endothelial cell lines from the murine lung and subcutaneous sponge implants. Arteriosclerosis, Thrombosis, and Vascular Biology. 1997;17:1599-1604.

70. Kleyman TR, Cragoe EJ. Amiloride and its analogs as tools in the study of ion transport. Journal of Membrane Biology. 1988;105:1-21.

71. Muro S, Mateescu M, Gajewski C, Robinson M, Muzykantov VR, Koval M. Control of intracellular trafficking of ICAM-1-targeted nanocarriers by endothelial Na^+/H^+ exchanger proteins. American Journal of Physiology, Lung Cellular and Molecular Physiology. 2006;290:L809-817.

72. Shaw SK, Perkins BN, Lim YC, et al. Reduced expression of junctional adhesion molecule and platelet/endothelial cell adhesion molecule-1 (CD31) at human

vascular endothelial junctions by cytokines tumor necrosis factor-α plus interferon-γ Does not reduce leukocyte transmigration under flow. American Journal of Pathology. 2001;159:2281-2291.

73. Allingham MJ, van Buul JD, Burridge K. ICAM-1-mediated, Src- and Pyk2-dependent vascular endothelial cadherin tyrosine phosphorylation is required for leukocyte transendothelial migration. The Journal of Immunology. 2007;179:4053-4064.

74. Barreiro O, Zamai M, Yáñez-Mó M, et al. Endothelial adhesion receptors are recruited to adherent leukocytes by inclusion in preformed tetraspanin nanoplatforms. The Journal of Cell Biology. 2008;183:527-542.

75. Zeidan YH, Jenkins RW, Hannun YA. Remodeling of cellular cytoskeleton by the acid sphingomyelinase/ceramide pathway. The Journal of Cell Biology. 2008;181:335-350.

76. Holopainen JM, Subramanian M, Kinnunen PK. Sphingomyelinase induces lipid microdomain formation in a fluid phosphatidylcholine/sphingomyelin membrane. Biochemistry. 1998;37:17562-17570.

77. Holopainen JM, Angelova MI, Kinnunen PK. Vectorial budding of vesicles by asymmetrical enzymatic formation of ceramide in giant liposomes. Biophysical Journal. 2000;78:830-838.

78. Zha X, Pierini LM, Leopold PL, Skiba PJ, Tabas I, Maxfield FR. Sphingomyelinase treatment induces ATP-independent endocytosis. The Journal of Cell Biology. 1998;140:39-47.

79. Bourguignon LYW, Singleton PA, Diedrich F, Stern R, Gilad E. CD44 interaction with Na^+-H^+ exchanger (NHE1) creates acidic microenvironments leading to hyaluronidase-2 and cathepsin B activation and breast tumor cell invasion. The Journal of Biological Chemistry. 2004;279:26991-27007.

80. Jenkins RW, Canals D, Hannun YA. Roles and regulation of secretory and lysosomal acid sphingomyelinase. Cell Signal. 2009;21:836-846.

81. Willingham MC, Pastan IH, Sahagian GG, Jourdian GW, Neufeld EF. Morphologic study of the internalization of a lysosomal enzyme by the mannose 6-phosphate receptor in cultured Chinese hamster ovary cells. Proceedings of the National Academy of Sciences USA. 1981;78:6967-6971.

82. Garnacho C, Shuvaev V, Thomas A, et al. RhoA activation and actin reorganization involved in endothelial CAM-mediated endocytosis of anti-PECAM carriers: critical role for tyrosine 686 in the cytoplasmic tail of PECAM-1. Blood. 2008;111:3024-3033.

83. Phillipson M, Heit B, Colarusso P, Liu L, Ballantyne CM, Kubes P. Intraluminal crawling of neutrophils to emigration sites: a molecularly distinct process from adhesion in the recruitment cascade. The Journal of Experimental Medicine. 2006;203:2569-2575.

84. Gérard A, van der Kammen RA, Janssen H, Ellenbroek SI, Collard JG. The Rac activator Tiam1 controls efficient T-cell trafficking and route of transendothelial migration. Blood. 2009;113:6138-6147.

85. Marmon S, Hinchey J, Oh P, et al. Caveolin-1 expression determines the route of neutrophil extravasation through skin microvasculature. American Journal of Pathology. 2009;174:684-692.

86. Denker SP, Huang DC, Orlowski J, Furthmayr H, Barber DL. Direct binding of the Na–H exchanger NHE1 to ERM proteins regulates the cortical cytoskeleton and cell shape independently of H^+ translocation. Molecular Cell. 2000;6:1425-1436.

87. Lagana A, Vadnais J, Le PU, et al. Regulation of the formation of tumor cell pseudopodia by the Na^+/H^+ exchanger NHE1. Journal of Cell Science. 2000;113 (Pt 20):3649-3662.

88. Hillebrand U, Hausberg M, Stock C, et al. 17β-estradiol increases volume, apical surface and elasticity of human endothelium mediated by Na^+/H^+ exchange. Cardiovascular Research. 2006;69:916-924.

89. Silva LC, Futerman AH, Prieto M. Lipid raft composition modulates sphingomyelinase activity and ceramide-induced membrane physical alterations. Biophysical Journal. 2009;96:3210-3222.

90. Tam C, Idone V, Devlin C, et al. Exocytosis of acid sphingomyelinase by wounded cells promotes endocytosis and plasma membrane repair. The Journal of Cell Biology. 2010;189:1027-1038.

91. Mebarek S, Komati H, Naro F, et al. Inhibition of *de novo* ceramide synthesis upregulates phospholipase D and enhances myogenic differentiation. Journal of Cell Science. 2007;120:407-416.

92. Utermöhlen O, Herz J, Schramm M, Krönke M. Fusogenicity of membranes: the impact of acid sphingomyelinase on innate immune responses. Immunobiology. 2008;213:307-314.

93. Rogasevskaia T, Coorssen JR. Sphingomyelin-enriched microdomains define the efficiency of native Ca^{2+}-triggered membrane fusion. Journal of Cell Science. 2006;119:2688-2694.

94. Andrews NW. Regulated secretion of conventional lysosomes. Trends in Cell Biology. 2000;10:316-321.

95. Altura BM, Gebrewold A, Zheng T, Altura BT. Sphingomyelinase and ceramide analogs induce vasoconstriction and leukocyte-endothelial interactions in cerebral venules in the intact rat brain: Insight into mechanisms and possible relation to brain injury and stroke. Brain Research Bulletin. 2002;58:271-278.

96. von Bismarck P, Wistädt C-FG, Klemm K, et al. Improved pulmonary function by acid sphingomyelinase inhibition in a newborn piglet lavage model. American Journal of Respiratory and Critical Care Medicine. 2008;177:1233-1241.

97. Teichgräber V, Ulrich M, Endlich N, et al. Ceramide accumulation mediates inflammation, cell death and infection susceptibility in cystic fibrosis. Nature Medicine. 2008;14:382-391.

98. Rebillard A, Tekpli X, Meurette O, et al. Cisplatin-induced apoptosis involves membrane fluidification via inhibition of NHE1 in human colon cancer cells. Cancer Research. 2007;67:7865-7874.

99. Xu H, Dawson R, Crane IJ, Liversidge J. Leukocyte diapedesis *in vivo* induces transient loss of tight junction protein at the blood-retina barrier. Investigative Ophthalmology & Visual Science. 2005;46:2487-2494.

100. Nash S, Stafford J, Madara JL. Effects of polymorphonuclear leukocyte transmigration on the barrier function of cultured intestinal epithelial monolayers. The Journal of Clinical Investigation. 1987;80:1104-1113.

101. Wedmore CV, Williams TJ. Control of vascular permeability by polymorphonuclear leukocytes in inflammation. Nature. 1981;289:646-650.

102. Vestweber D. VE-cadherin: the major endothelial adhesion molecule controlling cellular junctions and blood vessel formation. Arteriosclerosis, Thrombosis, and Vascular Biology. 2008;28:223-232.

103. Couture P, Paradis-Massie J, Oualha N, Thibault G. Adhesion and transcellular migration of neutrophils and B lymphocytes on fibroblasts. Experimental Cell Research. 2009;315:2192-2206.

104. Tabas I. Secretory sphingomyelinase. Chemistry and Physics of Lipids. 1999;102:123-130.

105. Wang G, Krishnamurthy K, Bieberich E. Regulation of primary cilia formation by ceramide. The Journal of Lipid Research. 2009;50:2103-2110.

106. Bollinger CR, Teichgräber V, Gulbins E. Ceramide-enriched membrane domains. Biochimica et Biophysica Acta. 2005;1746:284-294.

107. Lindner K, Uhlig U, Uhlig S. Ceramide alters endothelial cell permeability by a nonapoptotic mechanism. British Journal of Pharmacology. 2005;145:132-140.

108. Hauck CR, Grassmé H, Bock J, et al. Acid sphingomyelinase is involved in CEACAM receptor-mediated phagocytosis of *Neisseria gonorrhoeae*. FEBS Letters. 2000;478:260-266.

109. Grassmé H, Jendrossek V, Riehle A, et al. Host defense against *Pseudomonas aeruginosa* requires ceramide-rich membrane rafts. Nat Med. 2003;9:322-330.

110. Dreschers S, Franz P, Dumitru C, Wilker B, Jahnke K, Gulbins E. Infections with human rhinovirus induce the formation of distinct functional membrane domains. Cellular Physiology and Biochemistry. 2007;20:241-254.

111. Auerbach SD, Yang L, Luscinskas FW. Endothelial ICAM-1 functions in adhesion and signaling during leukocyte recruitment. Adhesion Molecules: Function and Inhibition. 2007:99-116.

112. Hopkins AM, Baird AW, Nusrat A. ICAM-1: targeted docking for exogenous as well as endogenous ligands. Advanced Drug Delivery Reviews. 2004;56:763-778.

113. Ockenhouse CF, Betageri R, Springer TA, Staunton DE. *Plasmodium falciparum*-infected erythrocytes bind ICAM-1 at a site distinct from LFA-1, Mac-1, and human rhinovirus. Cell. 1992;68:63-69.